

Utrecht University Repository

Title	Charged-particle multiplicity distributions over a wide pseudorapidity range in p–Pb collisions at $\sqrt{s_{NN}}=5.02$ TeV
Authors	ALICE Collaboration
Published in	European Physical Journal C
Publication Date	2025-08
Link	https://dspace.library.uu.nl/handle/1874/479085
Citation	ALICE Collaboration 2025, 'Charged-particle multiplicity distributions over a wide pseudorapidity range in p–Pb collisions at $\sqrt{s_{NN}}=5.02$ TeV', European Physical Journal C, vol. 85, no. 8, 919. https://doi.org/10.1140/epjc/s10052-025-14577-0
Versions / License	Publisher version
Rights	https://www.uu.nl/en/university-library/license-and-reuse-conditions



Charged-particle multiplicity distributions over a wide pseudorapidity range in p–Pb collisions at $\sqrt{s_{NN}} = 5.02$ TeV

ALICE Collaboration*

CERN, 1211 Geneva 23, Switzerland

Received: 10 March 2025 / Accepted: 24 July 2025
© CERN for the benefit of the ALICE Collaboration 2025

Abstract This paper presents the primary charged-particle multiplicity distributions in proton–lead collisions at a centre-of-mass energy per nucleon–nucleon collision of $\sqrt{s_{NN}} = 5.02$ TeV. The distributions are reported for non-single diffractive collisions in different pseudorapidity ranges. The measurements are performed using the combined information from the Silicon Pixel Detector and the Forward Multiplicity Detector of ALICE. The multiplicity distributions are parametrised with a double negative binomial distribution function which provides satisfactory descriptions of the distributions for all the studied pseudorapidity intervals. The data are compared to models and analysed quantitatively, evaluating the first four moments (mean, standard deviation, skewness, and kurtosis). The shape evolution of the measured multiplicity distributions is studied in terms of KNO variables and it is found that none of the considered models reproduces the measurements. This paper also reports on the average charged-particle multiplicity, normalised by the average number of participating nucleon pairs, as a function of the collision energy. The multiplicity results are then compared to measurements made in proton–proton and nucleus–nucleus collisions across a wide range of collision energies.

1 Introduction

The multiplicity distribution of primary charged particles, $P(N_{ch})$, is one of the key observables that provides valuable insights into the particle production mechanisms in high-energy hadronic and nuclear collisions. The production of charged particles at current collider energies involves the interplay of perturbative and non-perturbative quantum chromodynamic (QCD) interactions and is sensitive to colliding particle species, centre-of-mass energy, and collision centrality. ALICE measurements of charged-particle multiplicities across different collision systems over a broad range of pseudorapidity allow us to perform comprehensive stud-

ies of particle production at Large Hadron Collider (LHC) energies [1–8].

Recent experimental findings in proton–lead (p–Pb) collisions have shown characteristics of collectivity and strangeness enhancement that are typically attributed in heavy-ion collisions to the creation of a quark–gluon plasma (QGP) [9–13]. The origin of these phenomena is not yet fully understood, and it is crucial to investigate and understand the global properties of the system formed in p–Pb collisions, which makes the measurement of multiplicity distributions important. Moreover, the study of p–Pb collisions aids in understanding cold nuclear matter effects [14, 15] on the final-state particle production.

Following earlier ALICE results in proton–proton (pp) collisions [4], this paper presents, for the first time in p–Pb collisions at $\sqrt{s_{NN}} = 5.02$ TeV, a comprehensive set of measurements of $P(N_{ch})$ for the full phase space ($-3.4 < \eta_{lab} < 5.0$) and for a set of symmetric pseudorapidity ranges: $|\eta_{lab}| < 2.4$, $|\eta_{lab}| < 3.0$, and $|\eta_{lab}| < 3.4$. We also study the charged-particle production on both the p-fragmentation and the Pb-fragmentation sides in p–Pb collisions, covering pseudorapidity ranges: $-3.4 < \eta_{lab} < -1.0$ and $2.0 < \eta_{lab} < 5.0$, respectively. The results are compared to model calculations from HIJING (v1.36) [16], DPMJET (v3.0-5) [17], PYTHIA 8.308/Angantyr [18], and QCD saturation-based IP-Glasma [19, 20]. From the multiplicity distributions, we calculate the mean ($\langle N_{ch} \rangle$), standard deviation (σ), skewness (S), and kurtosis (κ) and compare them to the same moments evaluated from the considered models. This approach allows for a quantitative comparison of the performance of these models and provides input for their improved tuning to accurately simulate the underlying physics processes involved in particle production. This paper also reports a description of multiplicity distributions in terms of a double negative binomial distribution (NBD) function.

This article is organised as follows: Sect. 2 describes the experimental conditions, data sample considered in the analysis, the selection of collisions, and the reconstruction of

* e-mail: alice-publications@cern.ch

charged particles. Section 3 explains the correction procedure applied to the data. The estimates of systematic uncertainties from various sources are discussed in Sect. 4. Section 5 presents the results of this analysis, and, finally, the conclusions are summarised in Sect. 6.

2 Experimental details

The full description of the ALICE detectors and their performance can be found in dedicated publications [13, 21, 22]. The ALICE reference frame is defined with the z axis directed along the beam line and the nominal interaction point (IP) at $z = 0$. This analysis uses the data collected by ALICE in 2013 during the p–Pb collision run of the LHC. In these collisions, a proton beam with an energy of 4 TeV circulated towards the negative z direction ($\eta_{\text{lab}} < 0$), while lead ions with an energy of 1.58 TeV per nucleon circulated in the opposite direction ($\eta_{\text{lab}} > 0$). This configuration resulted in collisions at $\sqrt{s_{\text{NN}}} = 5.02$ TeV in the nucleon–nucleon centre-of-mass frame which is shifted in rapidity by $\Delta y = 0.465$ in the direction of the proton beam. In the following, the variable η_{lab} represents the pseudorapidity in the laboratory reference frame. The sub-detectors used in this analysis are briefly described below.

The V0 detector [23, 24] is made of two arrays of 32 scintillators: V0A, positioned at $z = 330$ cm and covering the pseudorapidity interval $2.8 < \eta_{\text{lab}} < 5.1$, and V0C, at $z = -90$ cm and covering $-3.7 < \eta_{\text{lab}} < -1.7$. Both the amplitude and the time of the signals produced by charged particles that hit each scintillator are recorded. The V0 detector is used for minimum-bias trigger selection and background rejection in this analysis.

The Silicon Pixel Detector (SPD) consists of the two innermost cylindrical layers of the ALICE Inner Tracking System (ITS) [22, 25] surrounding the central beryllium beam pipe. The SPD covers the pseudorapidity ranges $|\eta_{\text{lab}}| < 2$ and $|\eta_{\text{lab}}| < 1.4$ with full azimuthal coverage for the inner and outer layers, respectively. In this analysis, the SPD is used to determine the position of the interaction vertex and to estimate the charged-particle multiplicity around midrapidity ($|\eta_{\text{lab}}| < 2$).

The Forward Multiplicity Detector (FMD) [4, 6, 23] is a silicon strip detector composed of three sub-detectors placed at $z = 320$ cm (FMD1), 79 cm (FMD2), and -69 cm (FMD3). The FMD has full azimuthal coverage in the pseudorapidity ranges $-3.4 < \eta_{\text{lab}} < -1.7$ (FMD3) and $1.7 < \eta_{\text{lab}} < 5.0$ (FMD1 and FMD2), and these extend the charged-particle detection acceptance beyond the reach of the central detectors in ALICE.

A sample of non-single diffractive (NSD) collisions is selected using a minimum-bias (MB) trigger condition, which requires a coincidence between V0A and V0C time

signals. The standard ALICE collision selection criteria [26] is used in this analysis, which includes: rejection of background collisions such as beam–gas or beam–halo interactions that occur outside the interaction region, exclusion of pile-up collisions, and selection of the reconstructed primary vertex position (z_{vtx}) along z axis. However, in this analysis, the position of z_{vtx} is further restricted to be within ± 4 cm from the nominal IP to minimise the acceptance gaps in the pseudorapidity coverage of the SPD and FMD [4]. After applying all selection criteria, approximately 9 million p–Pb collisions are considered in this analysis.

The measurements of multiplicity at mid and forward rapidity are provided by the SPD and FMD, respectively. This analysis is focused on primary charged-particle measurements. Primary charged particles are defined as charged particles with a mean proper lifetime τ larger than $1 \text{ cm}/c$, which are either a) produced directly in the collision, or b) from decays of particles with τ smaller than $1 \text{ cm}/c$, excluding particles produced in interactions with material [27]. In the midrapidity region ($|\eta_{\text{lab}}| < 2$), charged particles can deposit energy and produce signals in more than one pixel of the SPD. The offline reconstruction combines such adjacent pixel signals into a single cluster. The clusters from the two layers of SPD, together with the primary vertex, are combined to form tracklets. The charged-particle multiplicity is then determined by counting the number of tracklets [28]. In the forward regions ($-3.4 < \eta_{\text{lab}} < -1.7$ and $1.7 < \eta_{\text{lab}} < 5.0$), the FMD records the energy deposited by charged particles that traverse each silicon strip. The number of charged particles per strip is then calculated using a statistical approach as described in Ref. [5]. When there is an overlap in the acceptance ($1.7 < |\eta_{\text{lab}}| < 2$) of the SPD and FMD, the multiplicity is determined by averaging the two measurements.

3 Correction procedure

As reported earlier, the main challenge in measuring the charged-particle multiplicity at forward rapidity is the significant background of secondary particles produced in interactions with the beam pipe and the material that exists in front of the FMD [4–6]. There are also other instrumental effects, such as detector acceptance and collision selection inefficiencies. A set of correction techniques is considered to account for these effects.

The main ingredients necessary to extract the primary charged-particle multiplicity distributions are the raw, uncorrected measured multiplicity distributions and a response matrix R . The matrix R is constructed via simulations where the known primary generated charged-particle multiplicity T is correlated with the simulated detector response M^s . Figure 1 shows a graphical representation of response matrix

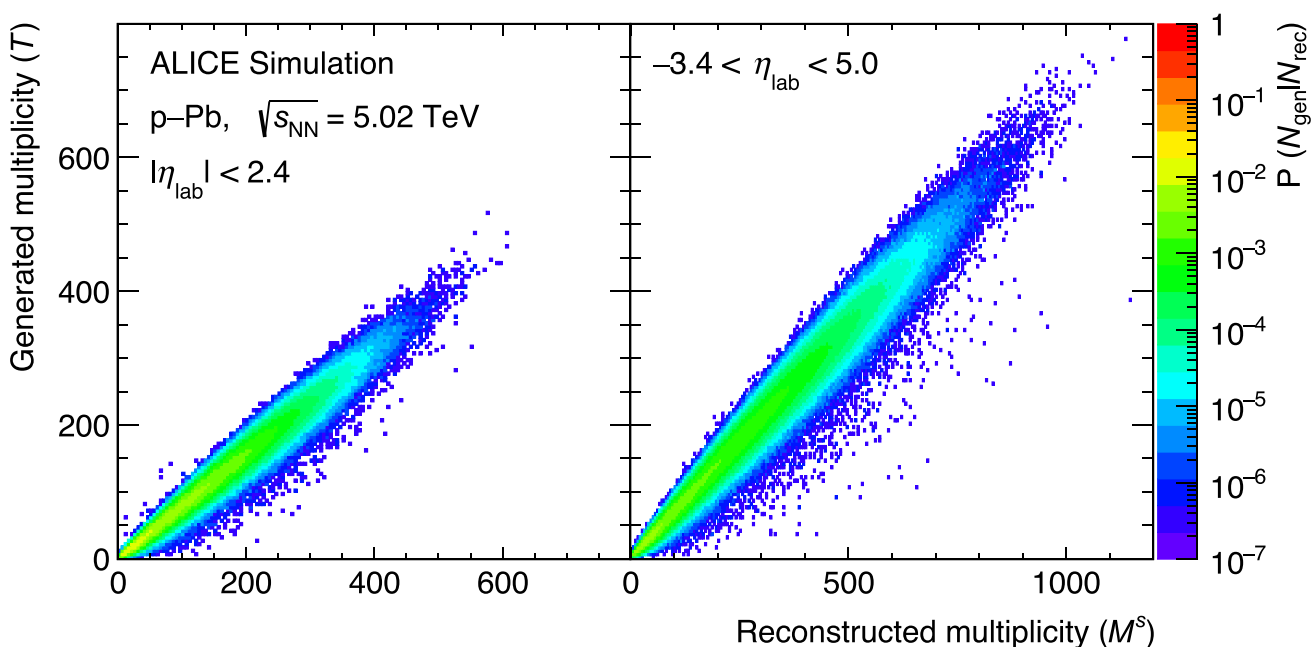


Fig. 1 Graphical representation of the detector response matrices obtained with the HIJING event generator for two pseudorapidity coverages: $|\eta_{\text{lab}}| < 2.4$ (left) and $-3.4 < \eta_{\text{lab}} < 5.0$ (right) in p–Pb collisions at $\sqrt{s_{\text{NN}}} = 5.02$ TeV

ces obtained with the HIJING event generator for the two pseudorapidity coverages: $|\eta_{\text{lab}}| < 2.4$ (left) and $-3.4 < \eta_{\text{lab}} < 5.0$ (right). The simulated detector response takes into account known conditions at the time of the data-taking, including inefficiencies, acceptance, electronic noise, and other smearing effects. Thus, one can write $M^S \approx RT$. The matrix element R_{mt} represents the conditional probability that an event with true multiplicity t is measured as an event with multiplicity m .

Experimentally, one needs to determine T for a given measured charged-particle distribution M . This can be symbolically written as

$$T = R^{-1}M. \tag{1}$$

However, the matrix R may be singular and cannot always be inverted analytically. Furthermore, even if R can be inverted, the results obtained with Eq. (1) contain oscillations mainly because of finite statistics in the response matrix. A regularised unfolding method based on Bayes’ theorem [29] using the RooUnfold software package [30] is used to overcome this problem.

The Bayesian unfolding technique is an iterative method in which the number of iterations serves as a regularisation parameter. Given an initial hypothesis (a prior), P_t , with $t = 1, \dots, n$, for the true distributions, Bayes’ theorem provides an estimation of the inverse matrix elements, \tilde{R}_{tm} ,

$$\tilde{R}_{tm} = \frac{R_{mt}P_t}{\sum_{t'} R_{mt'}P_{t'}}.$$

The unfolded distribution, U_t , is then obtained from

$$U_t = \sum_m \tilde{R}_{tm}M_m.$$

The obtained U_t is used as the prior distribution for the next iteration. After each iteration, the iterative process makes the unfolded distribution closer to the true one. In order to optimise the number of iterations, the χ^2/ndf between the unfolded and the true distribution is computed and then studied as a function of the number of iterations using MC simulations. The number of iterations is then set to the number for which the χ^2/ndf becomes minimum. The optimised number of iterations is found to be from 2 to 3 for the different pseudorapidity ranges. These number of iterations are used to unfold the experimental data to obtain the corrected multiplicity distributions.

The unfolded distributions are corrected further for the collision selection efficiency (ϵ), estimated via simulations as:

$$\epsilon = \frac{N_{\text{detected}}}{N_{\text{simulated}}},$$

where N_{detected} is the number of collisions detected by the simulated detector using NSD trigger condition with $|z_{\text{vtx}}| < 4$ cm and $N_{\text{simulated}}$ is the number of simulated NSD collisions with $|z_{\text{vtx}}| < 4$ cm. There is a dependence in the z_{vtx} distribution and selecting z_{vtx} introduces a bias in the efficiency. The effect is visible only for narrow vertex selections, and it is not relevant for $|z_{\text{vtx}}| < 4$ cm [4]. The values of ϵ are estimated as

Table 2 Contributions to systematic uncertainties (in percent) in the measurements of multiplicity distributions of primary charged particles on the p-fragmentation and the Pb-fragmentation sides in p–Pb collisions at $\sqrt{s_{NN}} = 5.02$ TeV. Numbers are given at three characteristic

multiplicity values of 2, the mean $\langle N_{ch} \rangle$, and the value for which $P(N_{ch}) = 10^{-3}$. Where the uncertainty is less than 0.1%, it is specified as ‘negl.’ in the table

Sources	$-3.4 < \eta_{lab} < -1.0$ (p-fragmentation side)			$2.0 < \eta_{lab} < 5.0$ (Pb-fragmentation side)		
	$N_{ch} = 2$	$N_{ch} = \langle N_{ch} \rangle$	$P(N_{ch}) = 10^{-3}$	$N_{ch} = 2$	$N_{ch} = \langle N_{ch} \rangle$	$P(N_{ch}) = 10^{-3}$
Upstream material	1.5	1.1	7.5	3.4	1.0	9.2
Event generator dependence	4.9	0.4	1.3	4.2	0.4	3.5
Unfolding parameters	1.7	negl.	0.2	2.7	0.1	0.1
Collision selection efficiency	1.0	negl.	negl.	8.9	negl.	negl.
Charged-particle detection thresholds	1.7	0.3	1.4	2.2	1.2	3.7
Total	5.7	1.0	7.7	11.0	1.6	10.5

unknown distribution and assign that as a systematic uncertainty due to the imprecise knowledge of the material in front of the detectors.

To determine the systematic uncertainty due to the event generator’s dependence on the unfolding procedure, the measured distributions in data are unfolded using two separate response matrices built using HIJING and DPMJET. The average of these two unfolded distributions is used as our final measurement. The resulting difference between the average value and the unfolded distributions obtained using HIJING and DPMJET is assigned as the systematic uncertainty. As described in Sect. 3, the unfolding of measured distributions is sensitive to the choice of the number of iterations in the Bayesian unfolding procedure. To account for this, unfolded distributions are obtained by varying the number of iterations by ± 1 around the optimised values. The deviations of these modified unfolded results from the nominal ones are considered as the systematic uncertainty.

The systematic uncertainty associated with the correction for the collision selection efficiency is evaluated by determining the efficiency values using two different event generators, HIJING and DPMJET. This uncertainty is largest at low multiplicity values and reduces significantly at larger N_{ch} because contributions from diffractive processes become smaller when going to higher multiplicity [1, 3, 4].

Depending on the incident angle, a charged particle may deposit energy in more than one FMD strip [5]. Signals shared in the neighbouring strips are then merged based on specific thresholds: a lower threshold (T_{low}) for accepting a signal and an upper threshold (T_{high}) to consider a signal as isolated, i.e. all energy is deposited in a single strip. The lower threshold is defined by the noise level (n) in the detector as $T_{low} = xn$, where the factor x is typically varied by one unit to estimate the one sigma variance in N_{ch} . The upper threshold is set such that the probability of energy loss (Δ) exceeding T_{high} for a single minimum ionizing particle (1

MIP) is greater than 99% ($P(\Delta > T_{high}|1MIP) > 99\%$). This threshold is varied so that the probability increases or decreases by one standard deviation, thus estimating the variance of N_{ch} . In order to calculate the number of charged particles using a Poisson statistical approach, the strips in the FMD are divided into regions, and the number of empty strips is compared to the total number of strips in a given region. Strips with a signal below a given threshold are considered empty. This threshold is varied within the boundaries of fits to the energy loss spectra to evaluate the systematic uncertainty.

5 Results and discussion

The primary charged-particle multiplicity distributions are measured for NSD p–Pb collisions at $\sqrt{s_{NN}} = 5.02$ TeV in six bins of pseudorapidities: $-3.4 < \eta_{lab} < 5.0$, $|\eta_{lab}| < 3.4$, $|\eta_{lab}| < 3.0$, $|\eta_{lab}| < 2.4$, $-3.4 < \eta_{lab} < -1.0$, and $2.0 < \eta_{lab} < 5.0$. The results are presented in Fig. 2. In the widest pseudorapidity range, the multiplicity distribution reaches a maximum around $N_{ch} \approx 22$, while for $|\eta_{lab}| < 2.4$, the maximum occurs around $N_{ch} \approx 12$. Beyond the maxima, the distributions fall steeply over several orders of magnitude. The coloured bands represent the systematic uncertainties, and the statistical uncertainties are smaller than the marker size. The multiplicity distributions $P(N_{ch})$ are found to broaden as the η_{lab} range increases. These measurements extend the high-multiplicity reach with respect to the previous ALICE results of pp collisions both in the central [1–3] and forward rapidity [4] regions. The distributions for $-3.4 < \eta_{lab} < 5.0$, $|\eta_{lab}| < 3.0$, and $2.0 < \eta_{lab} < 5.0$ are scaled by a factor of 10 for clarity. The green lines show fits using a double Negative Binomial Distribution (NBD) function to the data, as discussed in the next subsection.

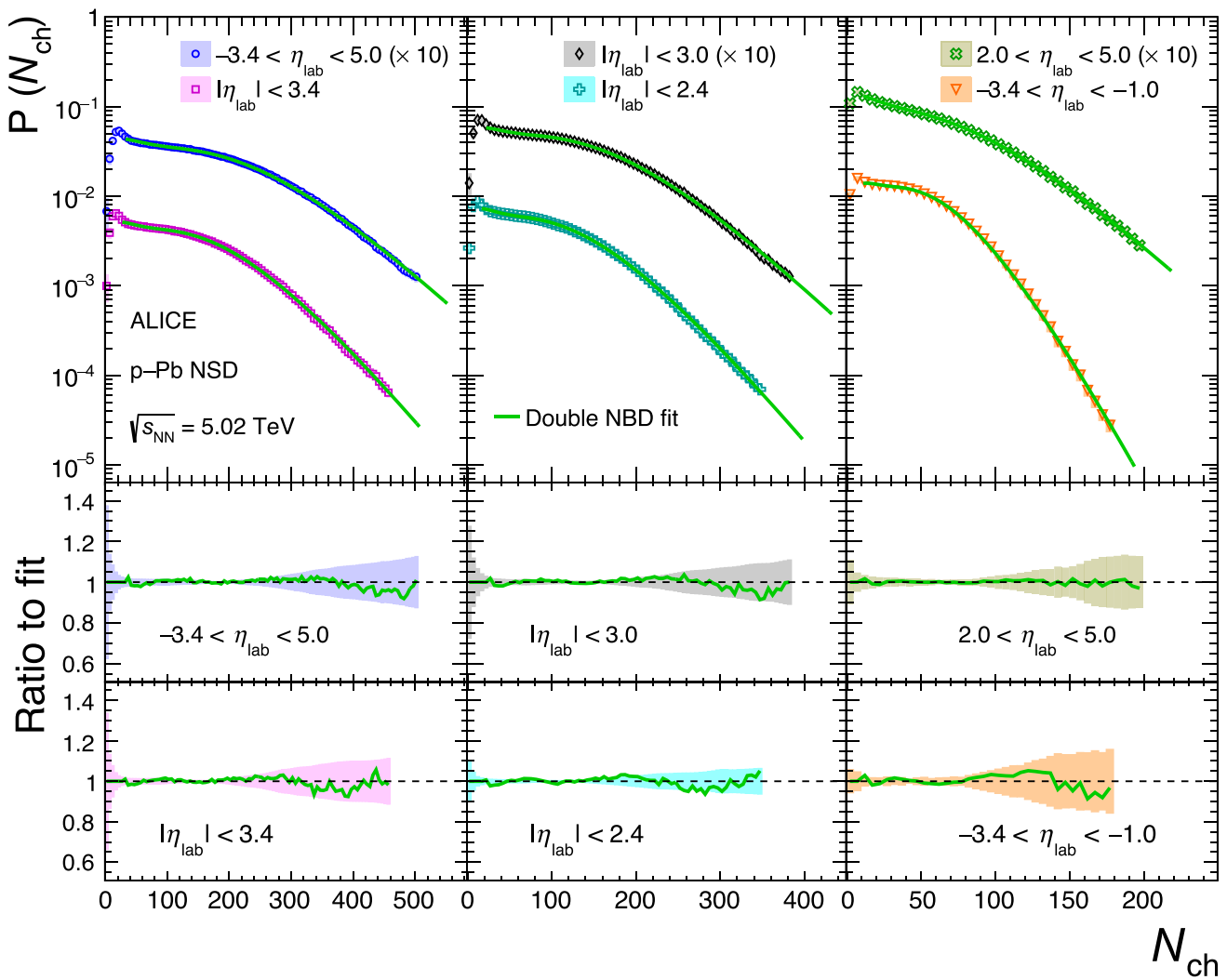


Fig. 2 Charged-particle multiplicity distributions for different pseudorapidity intervals measured in p–Pb collisions at $\sqrt{s_{\text{NN}}} = 5.02$ TeV for NSD collisions. The green lines show fits of a double NBD function to the data. The ratios of the data to the fits are shown in the bottom panels

5.1 Parametrisation of multiplicity distributions with double NBDs

Experimental measurements in pp ($p\bar{p}$) collisions at $\sqrt{s} \leq 2.36$ TeV for charged particles at midrapidity ($|\eta| < 1.5$) [1, 32, 33] have shown that the multiplicity distributions can be described by a single NBD given by the probability density function (p.d.f.)

$$f_{\text{NBD}}(n; \langle n \rangle, k) = \frac{\Gamma(n+k)}{\Gamma(k)\Gamma(n+1)} \frac{(\langle n \rangle/k)^n}{(1 + \langle n \rangle/k)^{n+k}}.$$

Here, $\langle n \rangle$ denotes the mean multiplicity and the parameter k is related to the standard deviation (σ) of the distribution by $\sigma/\langle n \rangle = \sqrt{1/\langle n \rangle + 1/k}$. However, at higher collision energies ($\sqrt{s} \geq 2.76$ TeV) and wider pseudorapidity intervals ($-3.4 < \eta < 5.0$), such a description is not adequate [2–4, 33]. Instead, those measurements are better captured by a

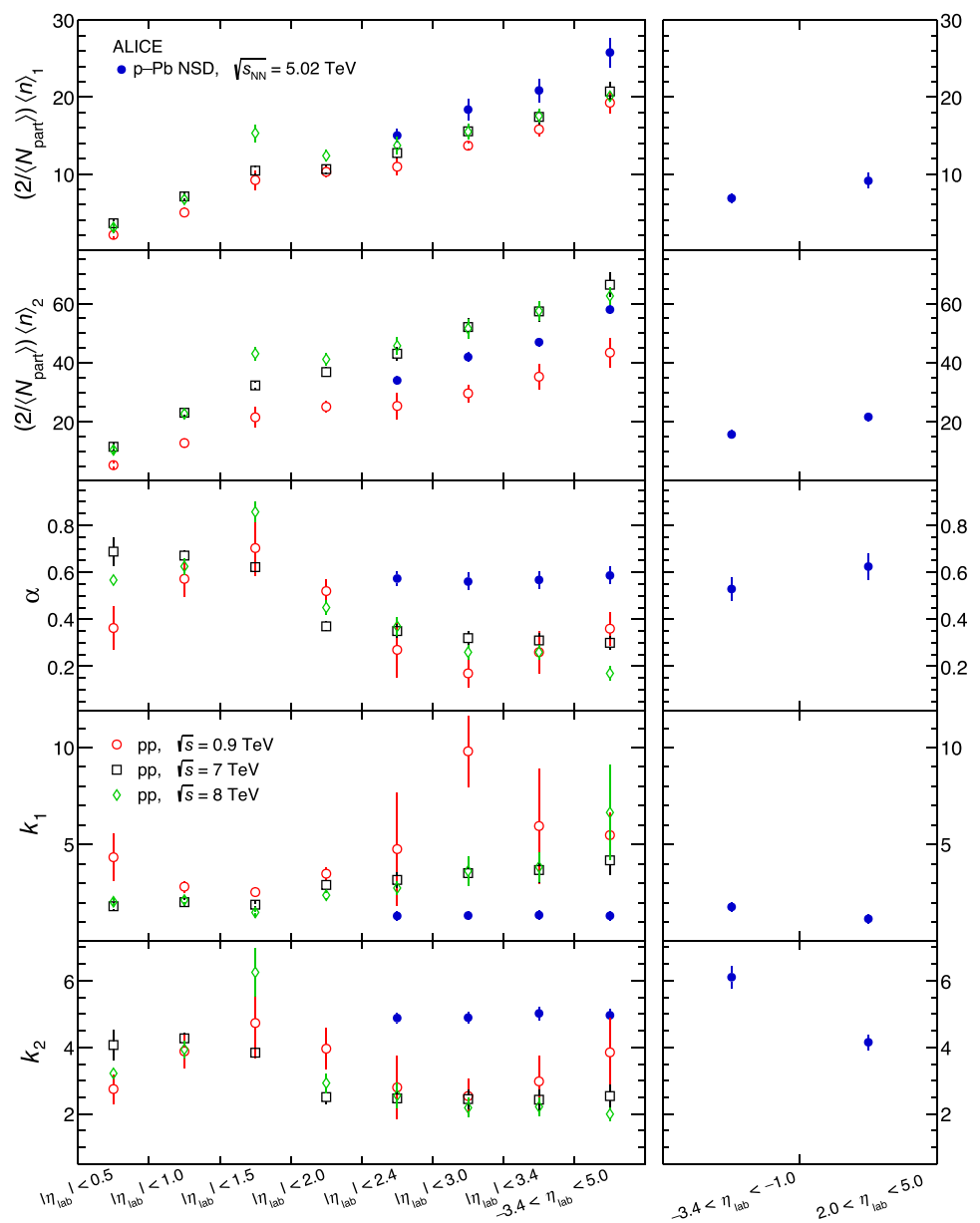
double NBD p.d.f. [3, 4, 33] given by

$$g(n; \langle n \rangle_1, k_1, \langle n \rangle_2, k_2, \lambda, \alpha) = \lambda[\alpha f_{\text{NBD}}(n; \langle n \rangle_1, k_1) + (1 - \alpha) f_{\text{NBD}}(n; \langle n \rangle_2, k_2)]. \quad (2)$$

In Eq. (2), $\langle n \rangle_1$ and $\langle n \rangle_2$ are the mean multiplicities of the first and second components (often interpreted as corresponding to soft and semihard processes), respectively, and the parameter α reflects the fraction of the first component [33–35]. The parameters k_1 and k_2 are related to the standard deviations of the distributions associated with the first and second components, respectively.

In this work, the double NBD p.d.f. (given by Eq. (2)) is fitted to the measured multiplicity distributions. The first few bins ($N_{\text{ch}} \approx 10$ to 30 depending on η window) of the multiplicity distributions are excluded from the fit and a free normalisation factor λ is introduced to account for this. This cut-off is chosen, primarily, to avoid the low-multiplicity

Fig. 3 The pseudorapidity dependence of the double NBD parameters: $\langle n \rangle_1$, $\langle n \rangle_2$, k_1 , and k_2 in p–Pb collisions at $\sqrt{s_{NN}} = 5.02$ TeV in comparison with pp measurements at $\sqrt{s} = 0.9, 7,$ and 8 TeV [3,4]. For p–Pb collisions, the $\langle n \rangle_1$ and $\langle n \rangle_2$ values are scaled by the $\langle N_{part} \rangle / 2$

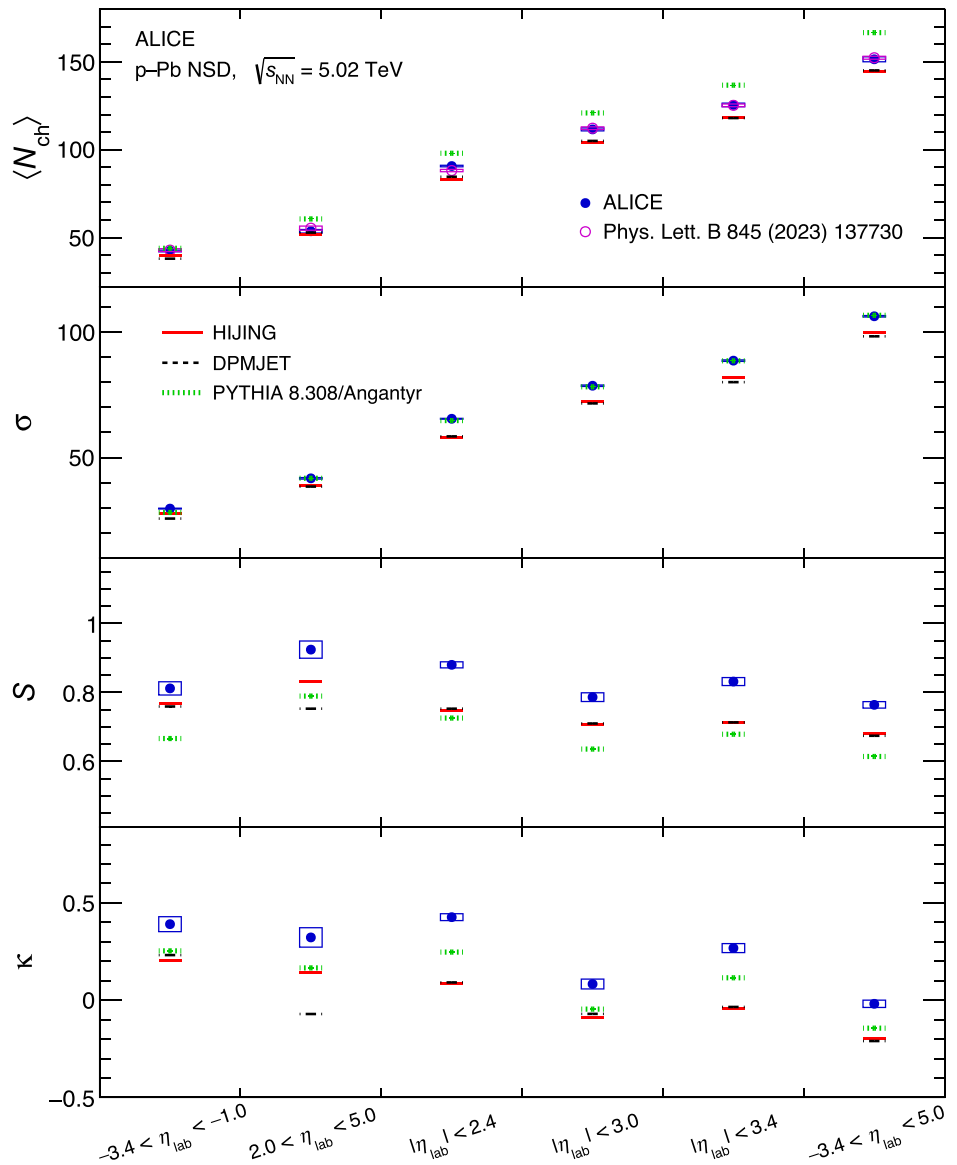


shape that is known to be not compatible with double NBD p.d.f. [3,4]. Coincidentally, diffractive contribution is only present at low multiplicities, however, there are no specific measurements available to estimate the importance of its effect on the shape of the multiplicity distribution. Nevertheless, it is expected that this contribution is well below the chosen cut-off as high-mass diffractive events that contribute to central multiplicity are quite rare. The fits are plotted together with the measured distributions in Fig. 2. The double NBD function reasonably describes the data within the uncertainties.

The obtained parameters from the fit to the data for different pseudorapidity intervals are shown in Fig. 3. The fit parameters obtained in p–Pb collisions are compared with the available pp measurements [3,4]. In p–Pb collisions, val-

ues of $\langle n \rangle_1$ and $\langle n \rangle_2$ are normalised by the average number of participating nucleon pairs ($\langle N_{part} \rangle / 2$). Both $\langle n \rangle_1$ and $\langle n \rangle_2$ increase with the increase in η_{lab} . It is found that $\langle n \rangle_2 \simeq 3\langle n \rangle_1$ for pp collisions at $\sqrt{s} = 7$ and 8 TeV whereas $\langle n \rangle_2 \simeq 2.4\langle n \rangle_1$ for pp collisions at $\sqrt{s} = 0.9$ TeV and p–Pb collisions at $\sqrt{s_{NN}} = 5.02$ TeV. This observation suggests a relationship between the two components of the multiplicity distribution, which may reflect the relative contributions from soft and semihard processes. In the left panels of Fig. 3, one can notice that for increasing pseudorapidity ranges starting at $|\eta_{lab}| < 2.4$, the normalised $\langle n \rangle_1^{p-Pb} \gtrsim \langle n \rangle_1^{pp}$ whereas the normalised $\langle n \rangle_2^{p-Pb}$ lies between the values observed at 0.9 and 7, 8 TeV for pp collisions. This suggests that the average multiplicity of the first (soft) component is nearly identical for both pp and p–Pb collisions, whereas the second

Fig. 4 Four moments: $\langle N_{\text{ch}} \rangle$, σ , S , and κ of charged-particle multiplicity distributions for different pseudorapidity intervals in p–Pb collisions at $\sqrt{s_{\text{NN}}} = 5.02$ TeV. Both skewness and kurtosis are plotted on two different ordinate scales to better visualize their respective variations. Predictions from the HIJING, DPMJET, and PYTHIA 8/Angantyr event generators are superimposed



(semihard) component follows an energy-dependent trend, increasing with energy. The parameters α , k_1 , and k_2 are independent of the width of the measured pseudorapidity interval for p–Pb collisions unlike in pp where they are found to have a mild dependence on the width of η_{lab} range. We observe clear differences in the NBD parameters of the multiplicity distributions between the p-fragmentation and the Pb-fragmentation sides (right panels of Fig. 3) in p–Pb collisions. The Pb-fragmentation side exhibits higher values of $\langle n \rangle_1$ and $\langle n \rangle_2$, likely due to increased particle production relative to the p-fragmentation side. In addition, both $\langle k \rangle_1$ and $\langle k \rangle_2$ are found to decrease from the p-fragmentation to the Pb-fragmentation side, while the parameter α is approximately similar for both sides.

5.2 Moments of the multiplicity distributions

To study multiplicity distributions and their shape, the first four moments ($\langle N_{\text{ch}} \rangle$, σ , S , and κ) are calculated. The obtained values of $\langle N_{\text{ch}} \rangle$, σ , S , and κ of the measured multiplicity distributions at different pseudorapidity intervals are shown in Fig. 4. The open boxes represent the systematic uncertainty and the statistical errors are smaller than the symbols. The values of $\langle N_{\text{ch}} \rangle$ and σ rise with the increasing width of the pseudorapidity interval. The expectation values of N_{ch} are also compared to those derived from previous ALICE $dN_{\text{ch}}/d\eta$ measurements [8] (open circles), which differ in methodology, and, consequently, have different uncertainties, albeit with some overlap. Both measurements are found to be consistent and have uncertainties of less than 1%, and overlapping uncertainties contribute no more than half of that

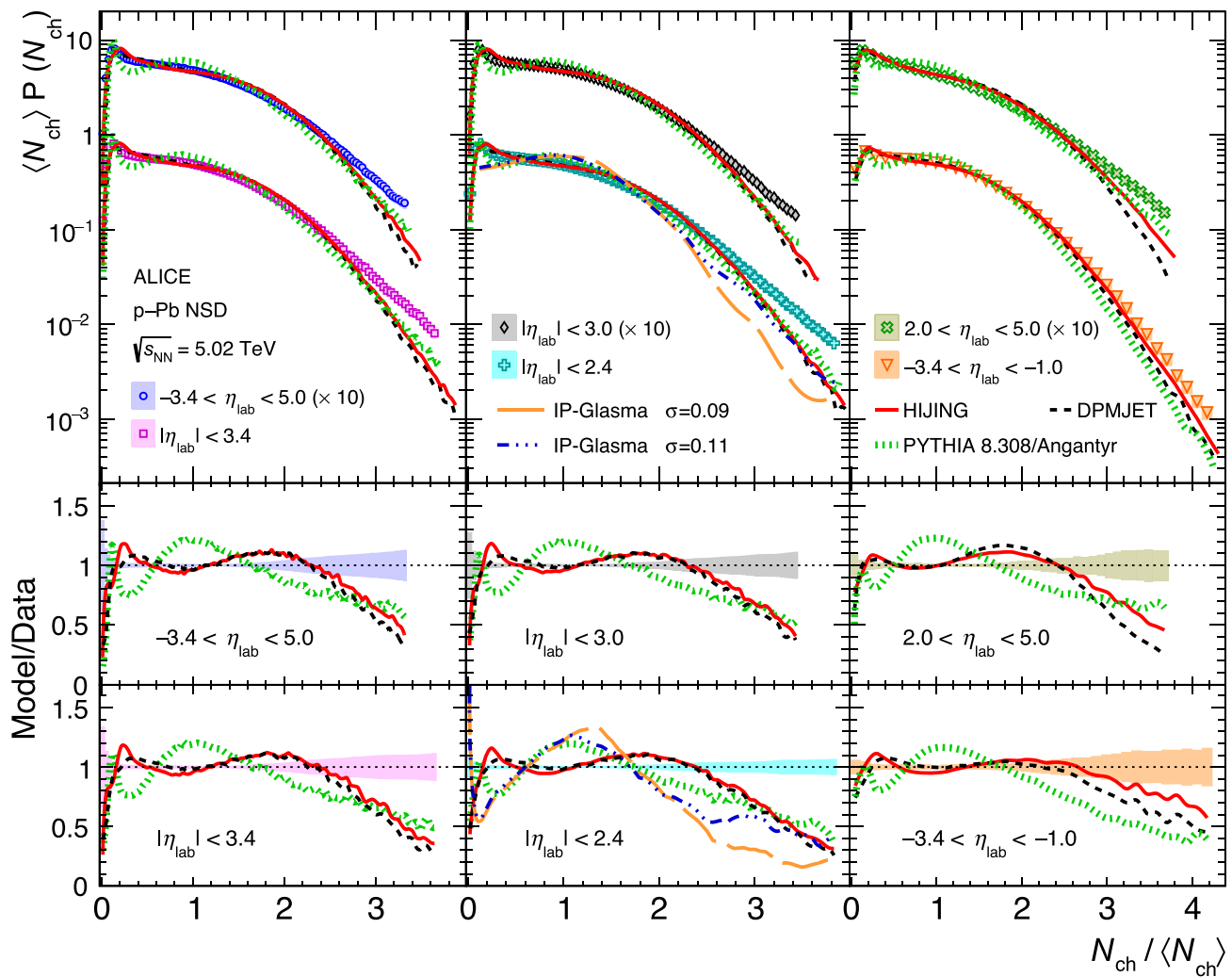


Fig. 5 KNO-scaled multiplicity distribution versus the KNO variable $N_{ch}/\langle N_{ch} \rangle$ in NSD p–Pb collisions at $\sqrt{s_{NN}} = 5.02$ TeV for various pseudorapidity intervals. Comparison with predictions from HIJING,

DPMJET, PYTHIA 8/Angantyr, and the IP-Glasma model are shown. The ratios between models and data are calculated using a linear interpolation between adjacent points

uncertainty. The skewness is positive, showing only a modest variation of approximately 0.2 across the studied η_{lab} intervals, while the kurtosis exhibits a weakly decreasing trend with increasing η_{lab} interval, changing by about 0.5. The different lines in Fig. 4 are predictions from the HIJING, DPMJET, and PYTHIA 8/Angantyr (default tune) event generators. The models follow the general trend of the data points; however, they show significant deviations from the data. The moments of the HIJING and DPMJET distributions are similar except the S and κ on the Pb-fragmentation side. The $\langle N_{ch} \rangle$ of the HIJING and DPMJET distributions are close to the data, but for the higher moments, they describe the data poorly, implying that the shape of their distributions is different from the data. On the other hand, PYTHIA 8/Angantyr reproduces the σ of the measured distributions but cannot

explain the rest of the moments (except the $\langle N_{ch} \rangle$ of the data on the p-fragmentation side).

5.3 KNO scaling in the multiplicity distributions

Koba, Nielsen and Olesen (KNO) found that for lower energy collisions, all moments of the multiplicity distribution scale with the first moment, i.e., $\langle N_{ch}^n \rangle \propto \langle N_{ch} \rangle^n$ [36]. Thus, a way to investigate properties of the multiplicity distributions is to plot these scaled by the mean multiplicity using the so-called KNO variable $N_{ch}/\langle N_{ch} \rangle$. This also has the added benefit that models that may differ in the mean of the distribution can still be compared to the empirical data. Figure 5 presents the data after scaling the probability density and the charged-particle multiplicity with the average number of charged particles $\langle N_{ch} \rangle$. The distributions for $-3.4 < \eta_{lab} < 5.0$, $|\eta_{lab}| < 3.0$,

and $2.0 < \eta_{\text{lab}} < 5.0$ are scaled by a factor of 10 for clarity. The data are compared with predictions from the HIJING, DPMJET, and PYTHIA 8/Angantyr event generators. The models underestimate the data both at low and high multiplicities, indicating that they give narrower distributions than the data. The HIJING and DPMJET distributions are close to one another and compatible with the data (within 10%) for $0.2 < N_{\text{ch}}/\langle N_{\text{ch}} \rangle < 2.5$. This indicates that HIJING and DPMJET provide similar $\langle N_{\text{ch}} \rangle$ values relative to data (also evident in the top panel of Fig. 4). On the other hand, PYTHIA 8/Angantyr gives the poorest description of the data in the intermediate multiplicities than the other two MC models. More specifically, PYTHIA 8/Angantyr is lower than the data for $0.2 < N_{\text{ch}}/\langle N_{\text{ch}} \rangle < 0.6$ while higher than the data for $0.6 < N_{\text{ch}}/\langle N_{\text{ch}} \rangle < 1.7$.

The measurement in $|\eta_{\text{lab}}| < 2.4$ is also compared to the prediction from the IP-Glasma model [37] based on the Color Glass Condensate (CGC) framework [38]. The IP-Glasma model incorporates fluctuations in the density of colour charges. In Fig. 5, the orange and blue distributions are generated with fluctuations of the colour charge density around the mean following a Gaussian distribution with width $\sigma = 0.09$ and 0.11 , respectively. The IP-Glasma model, irrespective of the size of the fluctuations, largely overestimates the data at very low multiplicities ($N_{\text{ch}}/\langle N_{\text{ch}} \rangle < 0.1$) and underestimates the same at high multiplicities ($N_{\text{ch}}/\langle N_{\text{ch}} \rangle > 2$).

5.4 System-size and energy dependence of $\langle N_{\text{ch}} \rangle$

In order to understand and compare the evolution of bulk particle production with collision energy and system-size, the mean charged-particle multiplicity is normalised by the $\langle N_{\text{part}} \rangle$ pairs and then presented as a function of $\sqrt{s_{\text{NN}}}$ in Fig. 6 for different collision systems. The $\langle N_{\text{ch}} \rangle$ is measured over a range more than eight units in pseudorapidity and the $\langle N_{\text{part}} \rangle$ is estimated using Glauber model calculations [7, 39–41]. Data from inelastic (INEL) and non-single diffractive pp ($p\bar{p}$) collisions [4, 39, 42] and central heavy-ion collisions [5–7] are shown for comparison. A power-law ($\alpha \cdot s_{\text{NN}}^\beta$) is fitted to the $\langle N_{\text{ch}} \rangle$ as a function of centre-of-mass energy. Best-fit parameter values are $\beta = 0.120 \pm 0.0001$, 0.127 ± 0.002 , and 0.192 ± 0.001 for INEL pp ($p\bar{p}$), NSD pp ($p\bar{p}$), and central AA collisions, respectively. The fit results are presented with their uncertainties shown by shaded bands. The results clearly show that the normalised $\langle N_{\text{ch}} \rangle$ increases faster with energy in central AA collisions than in pp collisions. The value of $\frac{2}{\langle N_{\text{part}} \rangle} \langle N_{\text{ch}} \rangle$ measured in p–Pb collisions at $\sqrt{s_{\text{NN}}} = 5.02$ TeV is half the magnitude of that in Pb–Pb collisions at the same energy, and falls on the INEL pp curve. A similar observation was also reported for charged-particle multiplicity measurements at midrapid-

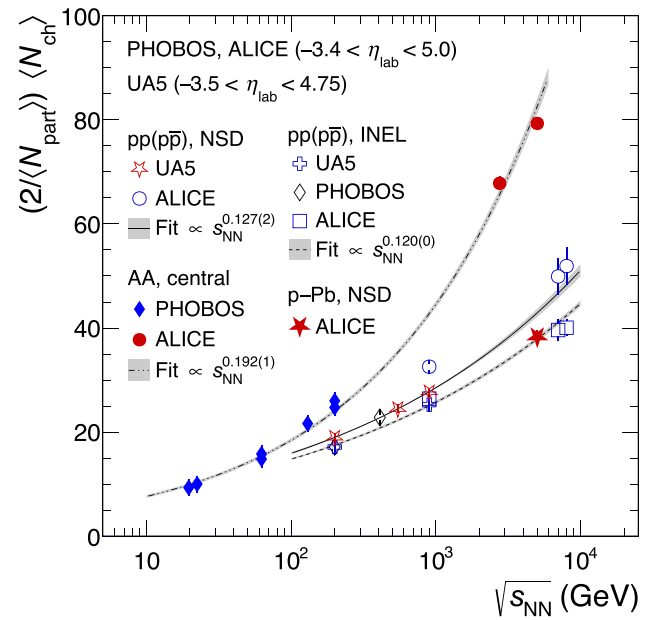


Fig. 6 Values of $\frac{2}{\langle N_{\text{part}} \rangle} \langle N_{\text{ch}} \rangle$ for minimum-bias pp [4, 39], $p\bar{p}$ [42], p–Pb and central AA [5–7] collisions as a function of $\sqrt{s_{\text{NN}}}$ are shown. The s_{NN} -dependencies of INEL pp ($p\bar{p}$) and NSD pp ($p\bar{p}$) collisions are proportional to $s_{\text{NN}}^{0.120}$ and $s_{\text{NN}}^{0.127}$ respectively. The results from central AA collisions are proportional to $s_{\text{NN}}^{0.192}$. The bands represent the uncertainties on the extracted power-law dependencies

ity ($|\eta_{\text{lab}}| < 0.5$) [26, 43, 44]. The similarity between the NSD p–Pb and the INEL pp data is yet to be understood.

6 Summary

The multiplicity distributions of primary charged particles have been measured in non-single diffractive p–Pb collisions at $\sqrt{s_{\text{NN}}} = 5.02$ TeV using the ALICE detector at the LHC. The measurements were performed over a wide pseudorapidity range ($-3.4 < \eta_{\text{lab}} < 5.0$), the widest possible among the four large LHC experiments. The multiplicity distributions are parametrised with a double Negative Binomial Distribution function, which describes the data well within the measurement uncertainties. The first four moments (mean, standard deviation, skewness, and kurtosis) of the multiplicity distributions are determined and compared with predictions from the HIJING, DPMJET, and PYTHIA 8/Angantyr MC event generators. HIJING and DPMJET describe the mean of the distribution within $\sim 5\%$ but cannot explain the higher moments of the data. On the other hand, PYTHIA 8/Angantyr reproduces only the second moment of the measured distributions but cannot describe the rest of the moments.

The multiplicity distributions are also presented as a function of the KNO variable and compared with predictions from HIJING, DPMJET, PYTHIA 8/Angantyr, and the CGC-based IP-Glasma model. None of the models can reproduce

the data in the reported multiplicity range. HIJING and DPMJET explain the data better than PYTHIA 8/Angantyr in the intermediate multiplicities. However, all MC predictions largely underestimate the multiplicity distributions at low and high multiplicities. The CGC-based IP-Glasma model disagrees with the measurements, irrespective of the level of colour charge fluctuations introduced into that model.

Finally, the dependence of $\frac{2}{\langle N_{\text{part}} \rangle} \langle N_{\text{ch}} \rangle$ on the centre-of-mass energy is parametrised by a power-law function, which shows that the multiplicity in p–Pb collisions coincides with the trend observed in inelastic pp collisions.

The measurements reported in this paper provide valuable information for better understanding particle production mechanisms in p–Pb collisions and offer valuable input for developing theoretical models and Monte Carlo event generators.

Acknowledgements The ALICE Collaboration would like to thank all its engineers and technicians for their invaluable contributions to the construction of the experiment and the CERN accelerator teams for the outstanding performance of the LHC complex. The ALICE Collaboration gratefully acknowledges the resources and support provided by all Grid centres and the Worldwide LHC Computing Grid (WLCG) collaboration. The ALICE Collaboration acknowledges the following funding agencies for their support in building and running the ALICE detector: A. I. Alikhanyan National Science Laboratory (Yerevan Physics Institute) Foundation (ANSL), State Committee of Science and World Federation of Scientists (WFS), Armenia; Austrian Academy of Sciences, Austrian Science Fund (FWF): [M 2467-N36] and Nationalstiftung für Forschung, Technologie und Entwicklung, Austria; Ministry of Communications and High Technologies, National Nuclear Research Center, Azerbaijan; Conselho Nacional de Desenvolvimento Científico e Tecnológico (CNPq), Financiadora de Estudos e Projetos (Finep), Fundação de Amparo à Pesquisa do Estado de São Paulo (FAPESP) and Universidade Federal do Rio Grande do Sul (UFRGS), Brazil; Bulgarian Ministry of Education and Science, within the National Roadmap for Research Infrastructures 2020-2027 (object CERN), Bulgaria; Ministry of Education of China (MOEC), Ministry of Science & Technology of China (MSTC) and National Natural Science Foundation of China (NSFC), China; Ministry of Science and Education and Croatian Science Foundation, Croatia; Centro de Aplicaciones Tecnológicas y Desarrollo Nuclear (CEADEN), Cubaenergía, Cuba; Ministry of Education, Youth and Sports of the Czech Republic, Czech Republic; The Danish Council for Independent Research | Natural Sciences, the VILLUM FONDEN and Danish National Research Foundation (DNRF), Denmark; Helsinki Institute of Physics (HIP), Finland; Commissariat à l’Energie Atomique (CEA) and Institut National de Physique Nucléaire et de Physique des Particules (IN2P3) and Centre National de la Recherche Scientifique (CNRS), France; Bundesministerium für Bildung und Forschung (BMBF) and GSI Helmholtzzentrum für Schwerionenforschung GmbH, Germany; General Secretariat for Research and Technology, Ministry of Education, Research and Religions, Greece; National Research, Development and Innovation Office, Hungary; Department of Atomic Energy Government of India (DAE), Department of Science and Technology, Government of India (DST), University Grants Commission, Government of India (UGC) and Council of Scientific and Industrial Research (CSIR), India; National Research and Innovation Agency - BRIN, Indonesia; Istituto Nazionale di Fisica Nucleare (INFN), Italy; Japanese Ministry of Education, Culture, Sports, Science and Technology (MEXT) and Japan Society for the Promotion of Science (JSPS) KAKENHI, Japan; Con-

sejo Nacional de Ciencia (CONACYT) y Tecnología, through Fondo de Cooperación Internacional en Ciencia y Tecnología (FONCICYT) and Dirección General de Asuntos del Personal Académico (DGAPA), Mexico; Nederlandse Organisatie voor Wetenschappelijk Onderzoek (NWO), Netherlands; The Research Council of Norway, Norway; Pontificia Universidad Católica del Perú, Peru; Ministry of Science and Higher Education, National Science Centre and WUT ID-UB, Poland; Korea Institute of Science and Technology Information and National Research Foundation of Korea (NRF), Republic of Korea; Ministry of Education and Scientific Research, Institute of Atomic Physics, Ministry of Research and Innovation and Institute of Atomic Physics and Universitatea Nationala de Stiinta si Tehnologie Politehnica Bucuresti, Romania; Ministry of Education, Science, Research and Sport of the Slovak Republic, Slovakia; National Research Foundation of South Africa, South Africa; Swedish Research Council (VR) and Knut & Alice Wallenberg Foundation (KAW), Sweden; European Organization for Nuclear Research, Switzerland; Suranaree University of Technology (SUT), National Science and Technology Development Agency (NSTDA) and National Science, Research and Innovation Fund (NSRF via PMU-B B05F650021), Thailand; Turkish Energy, Nuclear and Mineral Research Agency (TENMAK), Turkey; National Academy of Sciences of Ukraine, Ukraine; Science and Technology Facilities Council (STFC), United Kingdom; National Science Foundation of the United States of America (NSF) and United States Department of Energy, Office of Nuclear Physics (DOE NP), United States of America. In addition, individual groups or members have received support from: Czech Science Foundation (grant no. 23-07499S), Czech Republic; FORTE project, reg. no. CZ.02.01.01/00/22_008/0004632, Czech Republic, co-funded by the European Union, Czech Republic; European Research Council (grant no. 950692), European Union; Deutsche Forschungsgemeinschaft (DFG, German Research Foundation) “Neutrinos and Dark Matter in Astro- and Particle Physics” (grant no. SFB 1258), Germany; ICSC - National Research Center for High Performance Computing, Big Data and Quantum Computing and FAIR - Future Artificial Intelligence Research, funded by the NextGenerationEU program (Italy).

Data Availability Statement Data will be made available on reasonable request. [Authors’ comment: This manuscript has associated data in a HEPData repository at: <https://www.hepdata.net/record/ins2895567>.]

Code Availability Statement This manuscript has associated code/software. [Authors’ comment: The code/software used for the analysis is publicly available on the github repository, at the links <https://github.com/alisw/AlIRoot> and <https://github.com/alisw/AlIPhysics>.]

Open Access This article is licensed under a Creative Commons Attribution 4.0 International License, which permits use, sharing, adaptation, distribution and reproduction in any medium or format, as long as you give appropriate credit to the original author(s) and the source, provide a link to the Creative Commons licence, and indicate if changes were made. The images or other third party material in this article are included in the article’s Creative Commons licence, unless indicated otherwise in a credit line to the material. If material is not included in the article’s Creative Commons licence and your intended use is not permitted by statutory regulation or exceeds the permitted use, you will need to obtain permission directly from the copyright holder. To view a copy of this licence, visit <http://creativecommons.org/licenses/by/4.0/>.
Funded by SCOAP³.

References

1. ALICE Collaboration, K. Aamodt et al., Charged-particle multiplicity measurement in proton–proton collisions at $\sqrt{s} = 0.9$ and 2.36 TeV with ALICE at LHC. *Eur. Phys. J. C* **68**, 89–108 (2010). <https://doi.org/10.1140/epjc/s10052-010-1339-x>. [arXiv:1004.3034](https://arxiv.org/abs/1004.3034) [hep-ex]
2. ALICE Collaboration, K. Aamodt et al., Charged-particle multiplicity measurement in proton–proton collisions at $\sqrt{s} = 7$ TeV with ALICE at LHC. *Eur. Phys. J. C* **68**, 345–354 (2010). <https://doi.org/10.1140/epjc/s10052-010-1350-2>. [arXiv:1004.3514](https://arxiv.org/abs/1004.3514) [hep-ex]
3. ALICE Collaboration, J. Adam et al., Charged-particle multiplicities in proton–proton collisions at $\sqrt{s} = 0.9$ to 8 TeV. *Eur. Phys. J. C* **77**, 33 (2017). <https://doi.org/10.1140/epjc/s10052-016-4571-1>. [arXiv:1509.07541](https://arxiv.org/abs/1509.07541) [nucl-ex]
4. ALICE Collaboration, S. Acharya et al., Charged-particle multiplicity distributions over a wide pseudorapidity range in proton–proton collisions at $\sqrt{s} = 0.9, 7,$ and 8 TeV. *Eur. Phys. J. C* **77**, 852 (2017). <https://doi.org/10.1140/epjc/s10052-017-5412-6>. [arXiv:1708.01435](https://arxiv.org/abs/1708.01435) [hep-ex]
5. ALICE Collaboration, E. Abbas et al., Centrality dependence of the pseudorapidity density distribution for charged particles in Pb–Pb collisions at $\sqrt{s_{NN}} = 2.76$ TeV. *Phys. Lett. B* **726**, 610–622 (2013). <https://doi.org/10.1016/j.physletb.2013.09.022>. [arXiv:1304.0347](https://arxiv.org/abs/1304.0347) [nucl-ex]
6. ALICE Collaboration, J. Adam et al., Centrality evolution of the charged-particle pseudorapidity density over a broad pseudorapidity range in Pb–Pb collisions at $\sqrt{s_{NN}} = 2.76$ TeV. *Phys. Lett. B* **754**, 373–385 (2016). <https://doi.org/10.1016/j.physletb.2015.12.082>. [arXiv:1509.07299](https://arxiv.org/abs/1509.07299) [nucl-ex]
7. ALICE Collaboration, J. Adam et al., Centrality dependence of the pseudorapidity density distribution for charged particles in Pb–Pb collisions at $\sqrt{s_{NN}} = 5.02$ TeV. *Phys. Lett. B* **772**, 567–577 (2017). <https://doi.org/10.1016/j.physletb.2017.07.017>. [arXiv:1612.08966](https://arxiv.org/abs/1612.08966) [nucl-ex]
8. ALICE Collaboration, S. Acharya et al., System-size dependence of the charged-particle pseudorapidity density at $\sqrt{s_{NN}} = 5.02$ TeV for pp, p–Pb, and Pb–Pb collisions. *Phys. Lett. B* **845**, 137730 (2023). <https://doi.org/10.1016/j.physletb.2023.137730>. [arXiv:2204.10210](https://arxiv.org/abs/2204.10210) [nucl-ex]
9. ALICE Collaboration, B. Abelev et al., Long-range angular correlations on the near and away side in p–Pb collisions at $\sqrt{s_{NN}} = 5.02$ TeV. *Phys. Lett. B* **719**, 29–41 (2013). <https://doi.org/10.1016/j.physletb.2013.01.012>. [arXiv:1212.2001](https://arxiv.org/abs/1212.2001) [nucl-ex]
10. ATLAS Collaboration, G. Aad et al., Observation of associated near-side and away-side long-range correlations in $\sqrt{s_{NN}} = 5.02$ TeV p–Pb Collisions with the ATLAS Detector. *Phys. Rev. Lett.* **110**, 182302 (2013). <https://doi.org/10.1103/PhysRevLett.110.182302>. [arXiv:1212.5198](https://arxiv.org/abs/1212.5198) [hep-ex]
11. CMS Collaboration, S. Chatrchyan et al., Observation of long-range near-side angular correlations in p–Pb collisions at the LHC. *Phys. Lett. B* **718**, 795–814 (2013). <https://doi.org/10.1016/j.physletb.2012.11.025>. [arXiv:1210.5482](https://arxiv.org/abs/1210.5482) [nucl-ex]
12. ATLAS Collaboration, G. Aad et al., Measurement of long-range pseudorapidity correlations and azimuthal harmonics in $\sqrt{s_{NN}} = 5.02$ TeV p–Pb collisions with the ATLAS detector. *Phys. Rev. C* **90**, 044906 (2014). <https://doi.org/10.1103/PhysRevC.90.044906>. [arXiv:1409.1792](https://arxiv.org/abs/1409.1792) [hep-ex]
13. ALICE Collaboration, S. Acharya et al., The ALICE experiment: a journey through QCD. *Eur. Phys. J. C* **84**, 813 (2024). <https://doi.org/10.1140/epjc/s10052-024-12935-y>. [arXiv:2211.04384](https://arxiv.org/abs/2211.04384) [nucl-ex]
14. J.-W. Qiu, I. Vitev, Coherent QCD multiple scattering in proton–nucleus collisions. *Phys. Lett. B* **632**, 507–511 (2006). <https://doi.org/10.1016/j.physletb.2005.10.073>. [arXiv:hep-ph/0405068](https://arxiv.org/abs/hep-ph/0405068)
15. X.-N. Wang, X.-F. Guo, Multiple parton scattering in nuclei: parton energy loss. *Nucl. Phys. A* **696**, 788–832 (2001). [https://doi.org/10.1016/S0375-9474\(01\)01130-7](https://doi.org/10.1016/S0375-9474(01)01130-7). [arXiv:hep-ph/0102230](https://arxiv.org/abs/hep-ph/0102230)
16. X.-N. Wang, M. Gyulassy, HIJING: a Monte Carlo model for multiple jet production in pp, p-A and AA collisions. *Phys. Rev. D* **44**, 3501–3516 (1991). <https://doi.org/10.1103/PhysRevD.44.3501>
17. S. Roesler, R. Engel, J. Ranft, The Monte Carlo event generator DPMJET-III, in *International Conference on Advanced Monte Carlo for Radiation Physics, Particle Transport Simulation and Applications (MC 2000)*, pp. 1033–1038 (2000). https://doi.org/10.1007/978-3-642-18211-2_166. [arXiv:hep-ph/0012252](https://arxiv.org/abs/hep-ph/0012252)
18. C. Bierlich, G. Gustafson, L. Lönnblad, H. Shah, The Angantyr model for heavy-ion collisions in PYTHIA8. *JHEP* **10**, 134 (2018). [https://doi.org/10.1007/JHEP10\(2018\)134](https://doi.org/10.1007/JHEP10(2018)134). [arXiv:1806.10820](https://arxiv.org/abs/1806.10820) [hep-ph]
19. B. Schenke, P. Tribedy, R. Venugopalan, Fluctuating glasma initial conditions and flow in heavy ion collisions. *Phys. Rev. Lett.* **108**, 252301 (2012). <https://doi.org/10.1103/PhysRevLett.108.252301>. [arXiv:1202.6646](https://arxiv.org/abs/1202.6646) [nucl-th]
20. B. Schenke, P. Tribedy, R. Venugopalan, Event-by-event gluon multiplicity, energy density, and eccentricities in ultrarelativistic heavy-ion collisions. *Phys. Rev. C* **86**, 034908 (2012). <https://doi.org/10.1103/PhysRevC.86.034908>. [arXiv:1206.6805](https://arxiv.org/abs/1206.6805) [hep-ph]
21. ALICE Collaboration, K. Aamodt et al., The ALICE experiment at the CERN LHC. *JINST* **3**, S08002 (2008). <https://doi.org/10.1088/1748-0221/3/08/S08002>
22. ALICE Collaboration, B.B. Abelev et al., Performance of the ALICE experiment at the CERN LHC. *Int. J. Mod. Phys. A* **29**, 1430044 (2014). <https://doi.org/10.1142/S0217751X14300440>. [arXiv:1402.4476](https://arxiv.org/abs/1402.4476) [nucl-ex]
23. ALICE Collaboration, P. Cortese et al., ALICE forward detectors: FMD, T0 and V0: Technical Design Report. CERN-LHCC-2004-025. <https://cds.cern.ch/record/781854>
24. ALICE Collaboration, E. Abbas et al., Performance of the ALICE VZERO system. *JINST* **8**, P10016 (2013). <https://doi.org/10.1088/1748-0221/8/10/P10016>. [arXiv:1306.3130](https://arxiv.org/abs/1306.3130) [nucl-ex]
25. ALICE Collaboration, K. Aamodt et al., Alignment of the ALICE Inner Tracking System with cosmic-ray tracks. *JINST* **5**, P03003 (2010). <https://doi.org/10.1088/1748-0221/5/03/P03003>. [arXiv:1001.0502](https://arxiv.org/abs/1001.0502) [physics.ins-det]
26. ALICE Collaboration, B. Abelev et al., Pseudorapidity density of charged particles in p–Pb collisions at $\sqrt{s_{NN}} = 5.02$ TeV. *Phys. Rev. Lett.* **110**, 032301 (2013). <https://doi.org/10.1103/PhysRevLett.110.032301>. [arXiv:1210.3615](https://arxiv.org/abs/1210.3615) [nucl-ex]
27. ALICE Collaboration, S. Acharya et al., The ALICE definition of primary particles. ALICE-PUBLIC-2017-005. <https://cds.cern.ch/record/2270008>
28. ALICE Collaboration, K. Aamodt et al., Charged-particle multiplicity density at midrapidity in central Pb–Pb collisions at $\sqrt{s_{NN}} = 2.76$ TeV. *Phys. Rev. Lett.* **105**, 252301 (2010). <https://doi.org/10.1103/PhysRevLett.105.252301>. [arXiv:1011.3916](https://arxiv.org/abs/1011.3916) [nucl-ex]
29. G. D’Agostini, A multidimensional unfolding method based on Bayes’ theorem. *Nucl. Instrum. Methods Phys. Res., Sect. A* **362**, 487–498 (1995). [https://doi.org/10.1016/0168-9002\(95\)00274-X](https://doi.org/10.1016/0168-9002(95)00274-X)
30. T. Adye, Unfolding algorithms and tests using RooUnfold. [arXiv:1105.1160](https://arxiv.org/abs/1105.1160) [physics.data-an]
31. R. Barlow, Asymmetric systematic errors. *MAN-HEP-03-02*. [arXiv:physics/0306138](https://arxiv.org/abs/physics/0306138)
32. UA5 Collaboration, R.E. Ansorge et al., Charged-particle multiplicity distributions at 200 GeV and 900 GeV centre-of-mass energy. *Z. Phys. C* **43**, 357 (1989). <https://doi.org/10.1007/BF01506531>





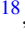






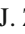
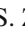
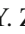



33. P. Ghosh, Negative binomial multiplicity distribution in proton-proton collisions in limited pseudorapidity intervals at LHC up to $\sqrt{s} = 7$ TeV and the clan model. *Phys. Rev. D* **85**, 054017 (2012). <https://doi.org/10.1103/PhysRevD.85.054017>. [arXiv:1202.4221](https://arxiv.org/abs/1202.4221) [hep-ph]
34. A. Giovannini, R. Ugoccioni, Possible scenarios for soft and semihard components structure in central hadron-hadron collisions in the TeV region. *Phys. Rev. D* **59**, 094020 (1999). <https://doi.org/10.1103/PhysRevD.59.094020>. [arXiv:hep-ph/9810446](https://arxiv.org/abs/hep-ph/9810446). [Erratum: *Phys. Rev. D* **69**, 059903 (2004)]
35. A. Giovannini, R. Ugoccioni, Possible scenarios for soft and semihard components structure in central hadron-hadron collisions in the TeV region: pseudorapidity intervals. *Phys. Rev. D* **60**, 074027 (1999). <https://doi.org/10.1103/PhysRevD.60.074027>. [arXiv:hep-ph/9905210](https://arxiv.org/abs/hep-ph/9905210)
36. Z. Koba, H.B. Nielsen, P. Olesen, Scaling of multiplicity distributions in high-energy hadron collisions. *Nucl. Phys. B* **40**, 317–334 (1972). [https://doi.org/10.1016/0550-3213\(72\)90551-2](https://doi.org/10.1016/0550-3213(72)90551-2)
37. B. Schenke, P. Tribedy, R. Venugopalan, Multiplicity distributions in pp, p-A and AA collisions from Yang-Mills dynamics. *Phys. Rev. C* **89**, 024901 (2014). <https://doi.org/10.1103/PhysRevC.89.024901>. [arXiv:1311.3636](https://arxiv.org/abs/1311.3636) [hep-ph]
38. E. Iancu, R. Venugopalan, *The Color Glass Condensate and High-energy Scattering in QCD* (World Scientific, Singapore, 2003). https://doi.org/10.1142/9789812795533_0005. [arXiv:hep-ph/0303204](https://arxiv.org/abs/hep-ph/0303204)
39. **PHOBOS** Collaboration, B. Alver et al., Phobos results on charged-particle multiplicity and pseudorapidity distributions in Au+Au, Cu+Cu, d+Au, and p+p collisions at ultra-relativistic energies. *Phys. Rev. C* **83**, 024913 (2011). <https://doi.org/10.1103/PhysRevC.83.024913>. [arXiv:1011.1940](https://arxiv.org/abs/1011.1940) [nucl-ex]
40. **ALICE** Collaboration, B. Abelev et al., Centrality determination of Pb–Pb collisions at $\sqrt{s_{NN}} = 2.76$ TeV with ALICE. *Phys. Rev. C* **88**, 044909 (2013). <https://doi.org/10.1103/PhysRevC.88.044909>. [arXiv:1301.4361](https://arxiv.org/abs/1301.4361) [nucl-ex]
41. **ALICE** Collaboration, J. Adam et al., Centrality dependence of particle production in p–Pb collisions at $\sqrt{s_{NN}} = 5.02$ TeV. *Phys. Rev. C* **91**, 064905 (2015). <https://doi.org/10.1103/PhysRevC.91.064905>. [arXiv:1412.6828](https://arxiv.org/abs/1412.6828) [nucl-ex]
42. **UA5** Collaboration, G.J. Alner et al., Scaling of pseudorapidity distributions at c.m. energies up to 0.9 TeV. *Z. Phys. C* **33**, 1–6 (1986). <https://doi.org/10.1007/BF01410446>
43. **ALICE** Collaboration, S. Acharya et al., Charged-particle pseudorapidity density at midrapidity in p–Pb collisions at $\sqrt{s_{NN}} = 8.16$ TeV. *Eur. Phys. J. C* **79**, 307 (2019). <https://doi.org/10.1140/epjc/s10052-019-6801-9>. [arXiv:1812.01312](https://arxiv.org/abs/1812.01312) [nucl-ex]
44. **CMS** Collaboration, A.M. Sirunyan et al., Pseudorapidity distributions of charged hadrons in p-Pb collisions at $\sqrt{s_{NN}} = 5.02$ and 8.16 TeV. *JHEP* **01**, 045 (2018). [https://doi.org/10.1007/JHEP01\(2018\)045](https://doi.org/10.1007/JHEP01(2018)045). [arXiv:1710.09355](https://arxiv.org/abs/1710.09355) [hep-ex]

ALICE Collaboration

S. Acharya⁵⁰, A. Agarwal¹³³, G. Aglieri Rinella³², L. Aglietta²⁴, M. Agnello²⁹, N. Agrawal²⁵, Z. Ahammed¹³³, S. Ahmad¹⁵, S. U. Ahn⁷¹, I. Ahuja³⁶, A. Akindinov¹³⁹, V. Akishina³⁸, M. Al-Turany⁹⁶, D. Aleksandrov¹³⁹, B. Alessandro⁵⁶, H. M. Alfanda⁶, R. Alfaro Molina⁶⁷, B. Ali¹⁵, A. Alici²⁵, N. Alizadehvandchali¹¹⁴, A. Alkin¹⁰³, J. Alme²⁰, G. Alocco²⁴, T. Alt⁶⁴, A. R. Altamura⁵⁰, I. Altsybeev⁹⁴, J. R. Alvarado⁴⁴, M. N. Anaam⁶, C. Andrei⁴⁵, N. Andreou¹¹³, A. Andronic¹²⁴, E. Andronov¹³⁹, V. Anguelov⁹³, F. Antinori⁵⁴, P. Antonioli⁵¹, N. Apadula⁷³, H. Appelshäuser⁶⁴, C. Arata⁷², S. Arcelli²⁵, R. Arnaldi⁵⁶, J. G. M. C. A. Arneiro¹⁰⁹, I. C. Arsene¹⁹, M. Arslanodk¹³⁶, A. Augustinus³², R. Averbeck⁹⁶, D. Averyanov¹³⁹, M. D. Azmi¹⁵, H. Baba¹²², A. Badalà⁵³, J. Bae¹⁰³, Y. Bae¹⁰³, Y. W. Baek⁴⁰, X. Bai¹¹⁸, R. Bailhache⁶⁴, Y. Bailung⁴⁸, R. Bala⁹⁰, A. Baldisseri¹²⁸, B. Balis², S. Bangalia¹¹⁶, Z. Banoo⁹⁰, V. Barbasova³⁶, F. Barile³¹, L. Barioglio⁵⁶, M. Barlou⁷⁷, B. Barman⁴¹, G. G. Barnaföldi⁴⁶, L. S. Barnby¹¹³, E. Barreau¹⁰², V. Barret¹²⁵, L. Barreto¹⁰⁹, K. Barth³², E. Bartsch⁶⁴, N. Bastid¹²⁵, S. Basu⁷⁴, G. Batigne¹⁰², D. Battistini⁹⁴, B. Batyunya¹⁴⁰, D. Bauri⁴⁷, J. L. Bazo Alba¹⁰⁰, I. G. Bearden⁸², P. Becht⁹⁶, D. Behera⁴⁸, I. Belikov¹²⁷, A. D. C. Bell Hechavarria¹²⁴, F. Bellini²⁵, R. Bellwied¹¹⁴, S. Belokurova¹³⁹, L. G. E. Beltran¹⁰⁸, Y. A. V. Beltran⁴⁴, G. Bencedi⁴⁶, A. Bensaoula¹¹⁴, S. Beole²⁴, Y. Berdnikov¹³⁹, A. Berdnikova⁹³, L. Bergmann⁹³, L. Bernardinis²³, L. Betev³², P. P. Bhaduri¹³³, A. Bhasin⁹⁰, B. Bhattacharjee⁴¹, S. Bhattarai¹¹⁶, L. Bianchi²⁴, J. Bielčik³⁴, J. Bielčíková⁸⁵, A. P. Bigot¹²⁷, A. Bilandzic⁹⁴, A. Binoy¹¹⁶, G. Biro⁴⁶, S. Biswas⁴, N. Bize¹⁰², J. T. Blair¹⁰⁷, D. Blau¹³⁹, M. B. Blidaru⁹⁶, N. Bluhme³⁸, C. Blume⁶⁴, F. Bock⁸⁶, T. Bodova²⁰, J. Bok¹⁶, L. Boldizsár⁴⁶, M. Bombara³⁶, P. M. Bond³², G. Bonomi^{55,132}, H. Borel¹²⁸, A. Borissov¹³⁹, A. G. Borquez Carcamo⁹³, E. Botta²⁴, Y. E. M. Bouziani⁶⁴, D. C. Brandibur⁶³, L. Bratrud⁶⁴, P. Braun-Munzinger⁹⁶, M. Bregant¹⁰⁹, M. Broz³⁴, G. E. Bruno^{31,95}, V. D. Buchakchiev³⁵, M. D. Buckland⁸⁴, D. Budnikov¹³⁹, H. Buesching⁶⁴, S. Bufalino²⁹, P. Buhler¹⁰¹, N. Burmasov¹³⁹, Z. Buthelezi^{68,121}, A. Bylinkin²⁰, S. A. Bysiak¹⁰⁶, J. C. Cabanillas Noris¹⁰⁸, M. F. T. Cabrera¹¹⁴, H. Caines¹³⁶, A. Caliva²⁸, E. Calvo Villar¹⁰⁰, J. M. M. Camacho¹⁰⁸, P. Camerini²³, M. T. Camerlingo⁵⁰, F. D. M. Canedo¹⁰⁹, S. Cannito²³, S. L. Cantway¹³⁶, M. Carabas¹¹², F. Carnesecchi³², L. A. D. Carvalho¹⁰⁹, J. Castillo Castellanos¹²⁸, M. Castoldi³², F. Catalano³², S. Cattaruzzi²³, R. Cerri²⁴, I. Chakaberia⁷³, P. Chakraborty¹³⁴, S. Chandra¹³³, S. Chapeland³², M. Chartier¹¹⁷, S. Chattopadhyay¹³³, M. Chen³⁹, T. Cheng⁶, C. Cheshkov¹²⁶, D. Chiappara²⁷, V. Chibante Barroso³², D. D. Chinellato¹⁰¹, F. Chinu²⁴, E. S. Chizzali^{94,a}, J. Cho⁵⁸, S. Cho⁵⁸, P. Chochula³², Z. A. Chochulska¹³⁴, D. Choudhury⁴¹, S. Choudhury⁹⁸, P. Christakoglou⁸³, C. H. Christensen⁸², P. Christiansen⁷⁴, T. Chujo¹²³, M. Ciacco²⁹, C. Cicalo⁵², G. Cimador²⁴, F. Cindolo⁵¹, M. R. Ciupek⁹⁶, G. Clai^{51,b}, F. Colamaria⁵⁰, J. S. Colburn⁹⁹, D. Colella³¹, A. Colelli³¹, M. Colocci²⁵, M. Concas³², G. Conesa Balbastre⁷², Z. Conesa del Valle¹²⁹, G. Contin²³, J. G. Contreras³⁴, M. L. Coquet¹⁰², P. Cortese^{56,131}, M. R. Cosentino¹¹¹, F. Costa³², S. Costanza²¹, P. Crochet¹²⁵, M. M. Czarnynoga¹³⁴, A. Dainese⁵⁴, G. Dange³⁸, M. C. Danisch⁹³, A. Danu⁶³, P. Das^{32,79}, S. Das⁴, A. R. Dash¹²⁴, S. Dash⁴⁷, A. De Caro²⁸, G. de Cataldo⁵⁰, J. de Cuveland³⁸, A. De Falco²², D. De Gruttola²⁸, N. De Marco⁵⁶, C. De Martin²³, S. De Pasquale²⁸, R. Deb¹³², R. Del Grande⁹⁴, L. Dello Stritto³², K. C. Devereaux¹⁸, G. G. A. de Souza¹⁰⁹, P. Dhankher¹⁸, D. Di Bari³¹, M. Di Costanzo²⁹, A. Di Mauro³², B. Di Ruzza¹³⁰, B. Diab¹²⁸, R. A. Diaz^{7,140}, Y. Ding⁶, J. Ditzel⁶⁴, R. Divià³², Ø. Djuvsland²⁰, U. Dmitrieva¹³⁹, A. Dobrin⁶³, B. Dönigus⁶⁴, J. M. Dubinski¹³⁴, A. Dubla⁹⁶, P. Dupieux¹²⁵, N. Dzalaiova¹³, T. M. Eder¹²⁴, R. J. Ehlers⁷³, F. Eisenhut⁶⁴, R. Ejima⁹¹, D. Elia⁵⁰, B. Erazmus¹⁰², F. Ercolessi²⁵, B. Espagnon¹²⁹, G. Eulisse³², D. Evans⁹⁹, S. Evdokimov¹³⁹, L. Fabbietti⁹⁴, M. Faggin³², J. Faivre⁷², F. Fan⁶, W. Fan⁷³, A. Fantoni⁴⁹, M. Fasel⁸⁶, G. Feofilov¹³⁹, A. Fernández Téllez⁴⁴, L. Ferrandi¹⁰⁹, M. B. Ferrer³², A. Ferrero¹²⁸, C. Ferrero^{56,c}, A. Ferretti²⁴, V. J. G. Feuillard⁹³, V. Filova³⁴, D. Finogeev¹³⁹, F. M. Fionda⁵², F. Flor¹³⁶, A. N. Flores¹⁰⁷, S. Foertsch⁶⁸, I. Fokin⁹³, S. Fokin¹³⁹, U. Follo^{56,c}, E. Fragiaco⁵⁷, E. Frajna⁴⁶, H. Fribert⁹⁴, U. Fuchs³², N. Funicello²⁸, C. Furget⁷², A. Furs¹³⁹, T. Fusayasu⁹⁷, J. J. Gaardhøje⁸², M. Gagliardi²⁴, A. M. Gago¹⁰⁰, T. Gahlaut⁴⁷, C. D. Galvan¹⁰⁸, S. Gami⁷⁹, D. R. Gangadharan¹¹⁴, P. Ganoti⁷⁷, C. Garabatos⁹⁶, J. M. Garcia⁴⁴, T. García Chávez⁴⁴, E. Garcia-Solis⁹, S. Garetti¹²⁹, C. Gargiulo³², P. Gasik⁹⁶, H. M. Gaur³⁸, A. Gautam¹¹⁶, M. B. Gay Ducati⁶⁶, M. Germain¹⁰², R. A. Gernhaeuser⁹⁴, C. Ghosh¹³³, M. Giacalone⁵¹, G. Gioachin²⁹, S. K. Giri¹³³, P. Giubellino^{56,96}, P. Giubileo²⁷, A. M. C. Glaenger¹²⁸, P. Glässel⁹³, E. Glimos¹²⁰, D. J. Q. Goh⁷⁵, V. Gonzalez¹³⁵, P. Gordeev¹³⁹, M. Gorgon², K. Goswami⁴⁸, S. Gotovac³³, V. Grabski⁶⁷, L. K. Graczykowski¹³⁴, E. Grecka⁸⁵, A. Grelli⁵⁹, C. Grigoras³², V. Grigoriev¹³⁹, S. Grigoryan^{1,140}, O. S. Groettvik³², F. Grosa³², J. F. Grosse-Oetringhaus³², R. Grosso⁹⁶, D. Grund³⁴, N. A. Grunwald⁹³

R. Guernane⁷² , M. Guilbaud¹⁰² , K. Gulbrandsen⁸² , J. K. Gumprecht¹⁰¹ , T. Gündem⁶⁴ , T. Gunji¹²² , J. Guo¹⁰ , W. Guo⁶ , A. Gupta⁹⁰ , R. Gupta⁹⁰ , R. Gupta⁴⁸ , K. Gwizdzziel¹³⁴ , L. Gyulai⁴⁶ , C. Hadjidakis¹²⁹ , F. U. Haider⁹⁰ , S. Haidlova³⁴ , M. Haldar⁴ , H. Hamagaki⁷⁵ , Y. Han¹³⁸ , B. G. Hanley¹³⁵ , R. Hannigan¹⁰⁷ , J. Hansen⁷⁴ , J. W. Harris¹³⁶ , A. Harton⁹ , M. V. Hartung⁶⁴ , H. Hassan¹¹⁵ , D. Hatzifotiadou⁵¹ , P. Hauer⁴² , L. B. Havener¹³⁶ , E. Hellbär³² , H. Helstrup³⁷ , M. Hemmer⁶⁴ , T. Herman³⁴ , S. G. Hernandez¹¹⁴ , G. Herrera Corral⁸ , S. Herrmann¹²⁶ , K. F. Hetland³⁷ , B. Heybeck⁶⁴ , H. Hillemanns³² , B. Hippolyte¹²⁷ , I. P. M. Hobus⁸³ , F. W. Hoffmann⁷⁰ , B. Hofman⁵⁹ , M. Horst⁹⁴ , A. Horzyk² , Y. Hou⁶ , P. Hristov³² , P. Huhn⁶⁴ , L. M. Huhta¹¹⁵ , T. J. Humanic⁸⁷ , A. Hutson¹¹⁴ , D. Hutter³⁸ , M. C. Hwang¹⁸ , R. Ilkaev¹³⁹ , M. Inaba¹²³ , M. Ippolitov¹³⁹ , A. Isakov⁸³ , T. Isidori¹¹⁶ , M. S. Islam^{47,98} , S. Iurchenko¹³⁹ , M. Ivanov¹³ , M. Ivanov⁹⁶ , V. Ivanov¹³⁹ , K. E. Iversen⁷⁴ , M. Jablonski² , B. Jacak^{18,73} , N. Jacazio²⁵ , P. M. Jacobs⁷³ , S. Jadlovská¹⁰⁵ , J. Jadlovsky¹⁰⁵ , S. Jaelani⁸¹ , C. Jahnke¹¹⁰ , M. J. Jakubowska¹³⁴ , M. A. Janik¹³⁴ , S. Ji¹⁶ , S. Jia¹⁰ , T. Jiang¹⁰ , A. A. P. Jimenez⁶⁵ , F. Jonas⁷³ , D. M. Jones¹¹⁷ , J. M. Jowett^{32,96} , J. Jung⁶⁴ , M. Jung⁶⁴ , A. Junique³² , A. Jusko⁹⁹ , J. Kaewjai¹⁰⁴ , P. Kalinak⁶⁰ , A. Kalweit³² , A. Karasu Uysal¹³⁷ , D. Karatovic⁸⁸ , N. Karatzenis⁹⁹ , O. Karavichev¹³⁹ , T. Karavicheva¹³⁹ , E. Karpechev¹³⁹ , M. J. Karwowska¹³⁴ , U. Kebschull⁷⁰ , M. Keil³² , B. Ketzer⁴² , J. Keul⁶⁴ , S. S. Khade⁴⁸ , A. M. Khan¹¹⁸ , S. Khan¹⁵ , A. Khanzadeev¹³⁹ , Y. Kharlov¹³⁹ , A. Khatun¹¹⁶ , A. Khuntia³⁴ , Z. Khuranova⁶⁴ , B. Kileng³⁷ , B. Kim¹⁰³ , C. Kim¹⁶ , D. J. Kim¹¹⁵ , D. Kim¹⁰³ , E. J. Kim⁶⁹ , J. Kim¹³⁸ , J. Kim⁵⁸ , J. Kim^{32,69} , M. Kim¹⁸ , S. Kim¹⁷ , T. Kim¹³⁸ , K. Kimura⁹¹ , S. Kirsch⁶⁴ , I. Kisel³⁸ , S. Kiselev¹³⁹ , A. Kisiel¹³⁴ , J. L. Klay⁵ , J. Klein³² , S. Klein⁷³ , C. Klein-Bösing¹²⁴ , M. Kleiner⁶⁴ , T. Klemenž⁹⁴ , A. Kluge³² , C. Kobdaj¹⁰⁴ , R. Kohara¹²² , T. Kollegger⁹⁶ , A. Kondratyev¹⁴⁰ , N. Kondratyeva¹³⁹ , J. König⁶⁴ , S. A. Königstorfer⁹⁴ , P. J. Konopka³² , G. Kornakov¹³⁹ , M. Korwieser⁹⁴ , S. D. Koryciak² , C. Koster⁸³ , A. Kotliarov⁸⁵ , N. Kovacic⁸⁸ , V. Kovalenko¹³⁹ , M. Kowalski¹⁰⁶ , V. Kozuharov³⁵ , G. Kozlov³⁸ , I. Králik⁶⁰ , A. Kravčáková³⁶ , L. Krcal³² , M. Krivda^{60,99} , F. Krizek⁸⁵ , K. Krizkova Gajdosova³⁴ , C. Krug⁶⁶ , M. Krüger⁶⁴ , D. M. Krupova³⁴ , E. Kryshen¹³⁹ , V. Kučera⁵⁸ , C. Kuhn¹²⁷ , P. G. Kuijjer⁸³ , T. Kumaoka¹²³ , D. Kumar¹³³ , L. Kumar⁸⁹ , N. Kumar⁸⁹ , S. Kumar⁵⁰ , S. Kundu³² , M. Kuo¹²³ , P. Kurashvili⁷⁸ , A. B. Kurepin¹³⁹ , A. Kuryakin¹³⁹ , S. Kushpil⁸⁵ , V. Kuskov¹³⁹ , M. Kutyla¹³⁴ , A. Kuznetsov¹⁴⁰ , M. J. Kweon⁵⁸ , Y. Kwon¹³⁸ , S. L. La Pointe³⁸ , P. La Rocca²⁶ , A. Lakrathok¹⁰⁴ , M. Lamanna³² , S. Lambert¹⁰² , A. R. Landou⁷² , R. Langoy¹¹⁹ , P. Larionov³² , E. Laudi³² , L. Lautner⁹⁴ , R. A. N. Laveaga¹⁰⁸ , R. Lavicka¹⁰¹ , R. Lea^{55,132} , H. Lee¹⁰³ , I. Legrand⁴⁵ , G. Legras¹²⁴ , A. M. Lejeune³⁴ , T. M. Lelek² , R. C. Lemmon^{84,*} , I. León Monzón¹⁰⁸ , M. M. Lesch⁹⁴ , P. Lévai⁴⁶ , M. Li⁶ , P. Li¹⁰ , X. Li¹⁰ , B. E. Liang-Gilman¹⁸ , J. Lien¹¹⁹ , R. Lietava⁹⁹ , I. Likmeta¹¹⁴ , B. Lim²⁴ , H. Lim¹⁶ , S. H. Lim¹⁶ , S. Lin¹⁰ , V. Lindenstruth³⁸ , C. Lippmann⁹⁶ , D. Liskova¹⁰⁵ , D. H. Liu⁶ , J. Liu¹¹⁷ , G. S. S. Liveraro¹¹⁰ , I. M. Lofnes²⁰ , C. Loizides⁸⁶ , S. Lokos¹⁰⁶ , J. Lömker⁵⁹ , X. Lopez¹²⁵ , E. López Torres⁷ , C. Lotteau¹²⁶ , P. Lu^{96,118} , W. Lu⁶ , Z. Lu¹⁰ , F. V. Lugo⁶⁷ , J. Luo³⁹ , G. Luparello⁵⁷ , Y. G. Ma³⁹ , M. Mager³² , A. Maire¹²⁷ , E. M. Majerz² , M. V. Makariev³⁵ , M. Malaev¹³⁹ , G. Malfattore^{25,51} , N. M. Malik⁹⁰ , N. Malik¹⁵ , S. K. Malik⁹⁰ , D. Mallick¹²⁹ , N. Mallick^{48,115} , G. Mandaglio^{30,53} , S. K. Mandal⁷⁸ , A. Manea⁶³ , V. Manko¹³⁹ , A. K. Manna⁴⁸ , F. Manso¹²⁵ , G. Mantzaridis⁹⁴ , V. Manzari⁵⁰ , Y. Mao⁶ , R. W. Marcjan² , G. V. Margagliotti²³ , A. Margotti⁵¹ , A. Marín⁹⁶ , C. Markert¹⁰⁷ , P. Martinengo³² , M. I. Martínez⁴⁴ , G. Martínez García¹⁰² , M. P. P. Martins^{32,109} , S. Masciocchi⁹⁶ , M. Masera²⁴ , A. Masoni⁵² , L. Massacrier¹²⁹ , O. Massen⁵⁹ , A. Mastroserio^{50,130} , L. Mattei^{24,125} , S. Mattiazzo²⁷ , A. Matyja¹⁰⁶ , F. Mazzaschi^{24,32} , M. Mazzilli¹¹⁴ , Y. Melikyan⁴³ , M. Melo¹⁰⁹ , A. Menchaca-Rocha⁶⁷ , J. E. M. Mendez⁶⁵ , E. Meninno¹⁰¹ , A. S. Menon¹¹⁴ , M. W. Menzel^{32,93} , M. Meres¹³ , L. Micheletti³² , D. Mihai¹¹² , D. L. Mihaylov⁹⁴ , A. U. Mikalsen²⁰ , K. Mikhaylov^{139,140}

H. Pei⁶, T. Peitzmann⁵⁹, X. Peng¹¹, M. Pennisi²⁴, S. Perciballi²⁴, D. Peresunko¹³⁹, G. M. Perez⁷, Y. Pestov¹³⁹, M. T. Petersen⁸², V. Petrov¹³⁹, M. Petrovici⁴⁵, S. Piano⁵⁷, M. Pikna¹³, P. Pillot¹⁰², L. O. D. L. Pimentel⁸², O. Pinazza^{32,51}, L. Pinsky¹¹⁴, C. Pinto³², S. Pisano⁴⁹, M. Płoskoń⁷³, M. Planinic⁸⁸, D. K. Plociennik², M. G. Poghosyan⁸⁶, B. Polichtchouk¹³⁹, S. Politano^{24,32}, N. Poljak⁸⁸, A. Pop⁴⁵, S. Porteboeuf-Houssais¹²⁵, V. Pozdniakov^{140,*}, I. Y. Pozos⁴⁴, K. K. Pradhan⁴⁸, S. K. Prasad⁴, S. Prasad⁴⁸, R. Preghenella⁵¹, F. Prino⁵⁶, C. A. Pruneau¹³⁵, I. Pshenichnov¹³⁹, M. Puccio³², S. Pucillo²⁴, S. Qiu⁸³, L. Quaglia²⁴, A. M. K. Radhakrishnan⁴⁸, S. Ragoni¹⁴, A. Rai¹³⁶, A. Rakotozafindrabe¹²⁸, N. Ramasubramanian¹²⁶, L. Ramello^{56,131}, C. O. Ramirez-Alvarez⁴⁴, M. Rasa²⁶, S. S. Räsänen⁴³, R. Rath⁵¹, M. P. Rauch²⁰, I. Ravasenga³², K. F. Read^{86,120}, C. Reckziegel¹¹¹, A. R. Redelbach³⁸, K. Redlich^{78,e}, C. A. Reetz⁹⁶, H. D. Regules-Medel⁴⁴, A. Rehman²⁰, F. Reidt³², H. A. Reme-Ness³⁷, K. Reygers⁹³, A. Riabov¹³⁹, V. Riabov¹³⁹, R. Ricci²⁸, M. Richter²⁰, A. A. Riedel⁹⁴, W. Riegler³², A. G. Riffero²⁴, M. Rignanese²⁷, C. Ripoli²⁸, C. Ristea⁶³, M. V. Rodriguez³², M. Rodríguez Cahuantzi⁴⁴, S. A. Rodríguez Ramírez⁴⁴, K. Røed¹⁹, R. Rogalev¹³⁹, E. Rogochaya¹⁴⁰, T. S. Rogoschinski⁶⁴, D. Rohr³², D. Röhrich²⁰, S. Rojas Torres³⁴, P. S. Rokita¹³⁴, G. Romanenko²⁵, F. Ronchetti³², D. Rosales Herrera⁴⁴, E. D. Rosas⁶⁵, K. Roslon¹³⁴, A. Rossi⁵⁴, A. Roy⁴⁸, S. Roy⁴⁷, N. Rubini⁵¹, J. A. Rudolph⁸³, D. Ruggiano¹³⁴, R. Rui²³, P. G. Russek², R. Russo⁸³, A. Rustamov⁸⁰, E. Ryabinkin¹³⁹, Y. Ryabov¹³⁹, A. Rybicki¹⁰⁶, L. C. V. Ryder¹¹⁶, J. Ryu¹⁶, W. Rzesza¹³⁴, B. Sabiu⁵¹, S. Sadhu⁴², S. Sadovsky¹³⁹, J. Saetre²⁰, S. Saha⁷⁹, B. Sahoo⁴⁸, R. Sahoo⁴⁸, D. Sahu⁴⁸, P. K. Sahu⁶¹, J. Saini¹³³, K. Sajdakova³⁶, S. Sakai¹²³, S. Sambyal⁹⁰, D. Samitz¹⁰¹, I. Sanna^{32,94}, T. B. Saramela¹⁰⁹, D. Sarkar⁸², P. Sarma⁴¹, V. Sarritzu²², V. M. Sarti⁹⁴, M. H. P. Sas³², S. Sawan⁷⁹, E. Scapparone⁵¹, J. Schambach⁸⁶, H. S. Scheid^{32,64}, C. Schiaua⁴⁵, R. Schicker⁹³, F. Schlepper^{32,93}, A. Schmah⁹⁶, C. Schmidt⁹⁶, M. O. Schmidt³², M. Schmidt⁹², N. V. Schmidt⁸⁶, A. R. Schmier¹²⁰, J. Schoengarth⁶⁴, R. Schotter¹⁰¹, A. Schröter³⁸, J. Schukraft³², K. Schweda⁹⁶, G. Scioli²⁵, E. Scomparin⁵⁶, J. E. Seger¹⁴, Y. Sekiguchi¹²², D. Sekihata¹²², M. Selina⁸³, I. Selyuzhenkov⁹⁶, S. Senyukov¹²⁷, J. J. Seo⁹³, D. Serebryakov¹³⁹, L. Serkin^{65,f}, L. Šerkšnytė⁹⁴, A. Sevcenco⁶³, T. J. Shaba⁶⁸, A. Shabetai¹⁰², R. Shahoyan³², A. Shangaraev¹³⁹, B. Sharma⁹⁰, D. Sharma⁴⁷, H. Sharma⁵⁴, M. Sharma⁹⁰, S. Sharma⁹⁰, U. Sharma⁹⁰, A. Shatat¹²⁹, O. Sheibani^{114,135}, K. Shigaki⁹¹, M. Shimomura⁷⁶, S. Shirinkin¹³⁹, Q. Shou³⁹, Y. Sibiriak¹³⁹, S. Siddhanta⁵², T. Siemiarzczuk⁷⁸, T. F. Silva¹⁰⁹, D. Silvermyr⁷⁴, T. Simantathammakul¹⁰⁴, R. Simeonov³⁵, B. Singh⁹⁰, B. Singh⁹⁴, K. Singh⁴⁸, R. Singh⁷⁹, R. Singh^{54,96}, S. Singh¹⁵, V. K. Singh¹³³, V. Singhal¹³³, T. Sinha⁹⁸, B. Sitar¹³, M. Sitta^{56,131}, T. B. Skaali¹⁹, G. Skorodumovs⁹³, N. Smirnov¹³⁶, R. J. M. Snellings⁵⁹, E.H. Solheim¹⁹, C. Sonnabend^{32,96}, J. M. Sonneveld⁸³, F. Soramel²⁷, A. B. Soto-Hernandez⁸⁷, R. Spijkers⁸³, I. Sputowska¹⁰⁶, J. Staa⁷⁴, J. Stachel⁹³, I. Stan⁶³, P. J. Steffanic¹²⁰, T. Stellhorn¹²⁴, S. F. Stiefelmaier⁹³, D. Stocco¹⁰², I. Storehaug¹⁹, N. J. Strangmann⁶⁴, P. Stratmann¹²⁴, S. Strazzi²⁵, A. Sturmiolo^{30,53}, C. P. Stylianidis⁸³, A. A. P. Suaide¹⁰⁹, C. Suire¹²⁹, A. Suiu^{32,112}, M. Sukhanov¹³⁹, M. Suljic³², R. Sultanov¹³⁹, V. Sumberia⁹⁰, S. Sumowidagdo⁸¹, L. H. Tabares⁷, S. F. Taghavi⁹⁴, J. Takahashi¹¹⁰, G.J. Tambave⁷⁹, S. Tang⁶, Z. Tang¹¹⁸, J. D. Tapia Takaki¹¹⁶, N. Tapus¹¹², L. A. Tarasovicova³⁶, M. G. Tarzila⁴⁵, A. Tauro³², A. Tavira García¹²⁹, G. Tejada Muñoz⁴⁴, L. Terlizzi²⁴, C. Terrevoli⁵⁰, D. Thakur²⁴, S. Thakur⁴, M. Thogersen¹⁹, D. Thomas¹⁰⁷, A. Tikhonov¹³⁹, N. Tiltmann^{32,124}, A. R. Timmins¹¹⁴, M. Tkacik¹⁰⁵, A. Toia⁶⁴, R. Tokumoto⁹¹, S. Tomassini²⁵, K. Tomohiro⁹¹, N. Topilskaya¹³⁹, M. Toppi⁴⁹, V. V. Torres¹⁰², A. Trifiro^{30,53}, T. Triloki⁹⁵, A. S. Triolo^{30,32,53}, S. Tripathy³², T. Tripathy^{47,125}, S. Trogolo²⁴, V. Trubnikov³, W. H. Trzaska¹¹⁵, T. P. Trzcinski¹³⁴, C. Tsolanta¹⁹, R. Tu³⁹, A. Tumkin¹³⁹, R. Turrisi⁵⁴, T. S. Tveter¹⁹, K. Ullaland²⁰, B. Ulukutlu⁹⁴, S. Upadhyaya¹⁰⁶, A. Uras¹²⁶, M. Urioni²³, G. L. Usai²², M. Vaid⁹⁰, M. Vala³⁶, N. Valle⁵⁵, L. V. R. van Doremalen⁵⁹, M. van Leeuwen⁸³, C. A. van Veen⁹³, R. J. G. van Weelden⁸³, D. Varga⁴⁶, Z. Varga^{46,136}, P. Vargas Torres⁶⁵, M. Vasileiou⁷⁷, A. Vasiliev^{139,*}, O. Vázquez Doce⁴⁹, O. Vazquez Rueda¹¹⁴, V. Vechernin¹³⁹, P. Veen¹²⁸, E. Vercellin²⁴, R. Verma⁴⁷, R. Vértesi⁴⁶, M. Verweij⁵⁹, L. Vickovic³³, Z. Vilakazi¹²¹, O. Villalobos Baillie⁹⁹, A. Villani²³, A. Vinogradov¹³⁹, T. Virgili²⁸, M. M. O. Virta¹¹⁵, A. Vodopyanov¹⁴⁰, B. Volkel³², M. A. Völkl⁹⁹, S. A. Voloshin¹³⁵, G. Volpe³¹, B. von Haller³², I. Vorobyev³², N. Vozniuk¹³⁹, J. Vrláková³⁶, J. Wan³⁹, C. Wang³⁹, D. Wang³⁹, Y. Wang³⁹, Y. Wang⁶, Z. Wang³⁹, A. Wegryzsek³², F. T. Weighofer³⁸, S. C. Wenzel³², J. P. Wessels¹²⁴, P. K. Wiacek², J. Wiechula⁶⁴, J. Wikne¹⁹, G. Wilk⁷⁸, J. Wilkinson⁹⁶, G. A. Willems¹²⁴, B. Windelband⁹³, M. Winn¹²⁸, J. R. Wright¹⁰⁷, W. Wu³⁹, Y. Wu¹¹⁸, K. Xiong³⁹, Z. Xiong¹¹⁸, R. Xu⁶, A. Yadav⁴², A. K. Yadav¹³³, Y. Yamaguchi⁹¹, S. Yang²⁰, S. Yano⁹¹, E. R. Yeats¹⁸, J. Yi⁶, Z. Yin⁶, I.-K. Yoo¹⁶, J. H. Yoon⁵⁸, H. Yu¹², S. Yuan²⁰, A. Yuncu⁹³, V. Zaccolo²³, C. Zampolli³², F. Zanone⁹³, N. Zardoshti³², A. Zarochentsev¹³⁹, P. Závada⁶², M. Zhalov¹³⁹, B. Zhang⁹³, C. Zhang¹²⁸, L. Zhang³⁹

M. Zhang^{6,125}, M. Zhang^{6,27}, S. Zhang³⁹, X. Zhang⁶, Y. Zhang¹¹⁸, Y. Zhang¹¹⁸, Z. Zhang⁶, M. Zhao¹⁰, V. Zhrebchevskii¹³⁹, Y. Zhi¹⁰, D. Zhou⁶, Y. Zhou⁸², J. Zhu^{6,54}, S. Zhu^{96,118}, Y. Zhu⁶, S. C. Zugravel⁵⁶, N. Zurlo^{55,132}

- ¹ A.I. Alikhanyan National Science Laboratory (Yerevan Physics Institute) Foundation, Yerevan, Armenia
- ² AGH University of Krakow, Cracow, Poland
- ³ Bogolyubov Institute for Theoretical Physics, National Academy of Sciences of Ukraine, Kiev, Ukraine
- ⁴ Department of Physics and Centre for Astroparticle Physics and Space Science (CAPSS), Bose Institute, Kolkata, India
- ⁵ California Polytechnic State University, San Luis Obispo, CA, USA
- ⁶ Central China Normal University, Wuhan, China
- ⁷ Centro de Aplicaciones Tecnológicas y Desarrollo Nuclear (CEADEN), Havana, Cuba
- ⁸ Centro de Investigación y de Estudios Avanzados (CINVESTAV), Mexico City and Mérida, Mexico
- ⁹ Chicago State University, Chicago, IL, USA
- ¹⁰ China Nuclear Data Center, China Institute of Atomic Energy, Beijing, China
- ¹¹ China University of Geosciences, Wuhan, China
- ¹² Chungbuk National University, Cheongju, Republic of Korea
- ¹³ Faculty of Mathematics, Physics and Informatics, Comenius University Bratislava, Bratislava, Slovak Republic
- ¹⁴ Creighton University, Omaha, NE, USA
- ¹⁵ Department of Physics, Aligarh Muslim University, Aligarh, India
- ¹⁶ Department of Physics, Pusan National University, Pusan, Republic of Korea
- ¹⁷ Department of Physics, Sejong University, Seoul, Republic of Korea
- ¹⁸ Department of Physics, University of California, Berkeley, CA, USA
- ¹⁹ Department of Physics, University of Oslo, Oslo, Norway
- ²⁰ Department of Physics and Technology, University of Bergen, Bergen, Norway
- ²¹ Dipartimento di Fisica, Università di Pavia, Pavia, Italy
- ²² Dipartimento di Fisica dell'Università and Sezione INFN, Cagliari, Italy
- ²³ Dipartimento di Fisica dell'Università and Sezione INFN, Trieste, Italy
- ²⁴ Dipartimento di Fisica dell'Università and Sezione INFN, Turin, Italy
- ²⁵ Dipartimento di Fisica e Astronomia dell'Università and Sezione INFN, Bologna, Italy
- ²⁶ Dipartimento di Fisica e Astronomia dell'Università and Sezione INFN, Catania, Italy
- ²⁷ Dipartimento di Fisica e Astronomia dell'Università and Sezione INFN, Padua, Italy
- ²⁸ Dipartimento di Fisica 'E.R. Caianiello' dell'Università and Gruppo Collegato INFN, Salerno, Italy
- ²⁹ Dipartimento DISAT del Politecnico and Sezione INFN, Turin, Italy
- ³⁰ Dipartimento di Scienze MIFT, Università di Messina, Messina, Italy
- ³¹ Dipartimento Interateneo di Fisica 'M. Merlin' and Sezione INFN, Bari, Italy
- ³² European Organization for Nuclear Research (CERN), Geneva, Switzerland
- ³³ Faculty of Electrical Engineering, Mechanical Engineering and Naval Architecture, University of Split, Split, Croatia
- ³⁴ Faculty of Nuclear Sciences and Physical Engineering, Czech Technical University in Prague, Prague, Czech Republic
- ³⁵ Faculty of Physics, Sofia University, Sofia, Bulgaria
- ³⁶ Faculty of Science, P.J. Šafárik University, Košice, Slovak Republic
- ³⁷ Faculty of Technology, Environmental and Social Sciences, Bergen, Norway
- ³⁸ Frankfurt Institute for Advanced Studies, Johann Wolfgang Goethe-Universität Frankfurt, Frankfurt, Germany
- ³⁹ Fudan University, Shanghai, China
- ⁴⁰ Gangneung-Wonju National University, Gangneung, Republic of Korea
- ⁴¹ Department of Physics, Gauhati University, Guwahati, India
- ⁴² Helmholtz-Institut für Strahlen- und Kernphysik, Rheinische Friedrich-Wilhelms-Universität Bonn, Bonn, Germany
- ⁴³ Helsinki Institute of Physics (HIP), Helsinki, Finland
- ⁴⁴ High Energy Physics Group, Universidad Autónoma de Puebla, Puebla, Mexico
- ⁴⁵ Horia Hulubei National Institute of Physics and Nuclear Engineering, Bucharest, Romania
- ⁴⁶ HUN-REN Wigner Research Centre for Physics, Budapest, Hungary
- ⁴⁷ Indian Institute of Technology Bombay (IIT), Mumbai, India

- 48 Indian Institute of Technology Indore, Indore, India
- 49 INFN, Laboratori Nazionali di Frascati, Frascati, Italy
- 50 INFN, Sezione di Bari, Bari, Italy
- 51 INFN, Sezione di Bologna, Bologna, Italy
- 52 INFN, Sezione di Cagliari, Cagliari, Italy
- 53 INFN, Sezione di Catania, Catania, Italy
- 54 INFN, Sezione di Padova, Padua, Italy
- 55 INFN, Sezione di Pavia, Pavia, Italy
- 56 INFN, Sezione di Torino, Turin, Italy
- 57 INFN, Sezione di Trieste, Trieste, Italy
- 58 Inha University, Incheon, Republic of Korea
- 59 Institute for Gravitational and Subatomic Physics (GRASP), Utrecht University/Nikhef, Utrecht, Netherlands
- 60 Institute of Experimental Physics, Slovak Academy of Sciences, Košice, Slovak Republic
- 61 Institute of Physics, Homi Bhabha National Institute, Bhubaneswar, India
- 62 Institute of Physics of the Czech Academy of Sciences, Prague, Czech Republic
- 63 Institute of Space Science (ISS), Bucharest, Romania
- 64 Institut für Kernphysik, Johann Wolfgang Goethe-Universität Frankfurt, Frankfurt, Germany
- 65 Instituto de Ciencias Nucleares, Universidad Nacional Autónoma de México, Mexico City, Mexico
- 66 Instituto de Física, Universidade Federal do Rio Grande do Sul (UFRGS), Porto Alegre, Brazil
- 67 Instituto de Física, Universidad Nacional Autónoma de México, Mexico City, Mexico
- 68 iThemba LABS, National Research Foundation, Somerset West, South Africa
- 69 Jeonbuk National University, Jeonju, Republic of Korea
- 70 Johann-Wolfgang-Goethe Universität Frankfurt Institut für Informatik, Fachbereich Informatik und Mathematik, Frankfurt, Germany
- 71 Korea Institute of Science and Technology Information, Daejeon, Republic of Korea
- 72 Laboratoire de Physique Subatomique et de Cosmologie, CNRS-IN2P3, Université Grenoble-Alpes, Grenoble, France
- 73 Lawrence Berkeley National Laboratory, Berkeley, CA, USA
- 74 Division of Particle Physics, Department of Physics, Lund University, Lund, Sweden
- 75 Nagasaki Institute of Applied Science, Nagasaki, Japan
- 76 Nara Women's University (NWU), Nara, Japan
- 77 Department of Physics, School of Science, National and Kapodistrian University of Athens, Athens, Greece
- 78 National Centre for Nuclear Research, Warsaw, Poland
- 79 National Institute of Science Education and Research, Homi Bhabha National Institute, Jatni, India
- 80 National Nuclear Research Center, Baku, Azerbaijan
- 81 National Research and Innovation Agency-BRIN, Jakarta, Indonesia
- 82 Niels Bohr Institute, University of Copenhagen, Copenhagen, Denmark
- 83 Nikhef, National institute for subatomic physics, Amsterdam, Netherlands
- 84 Nuclear Physics Group, STFC Daresbury Laboratory, Daresbury, UK
- 85 Nuclear Physics Institute of the Czech Academy of Sciences, Husinec-Řež, Czech Republic
- 86 Oak Ridge National Laboratory, Oak Ridge, TN, USA
- 87 Ohio State University, Columbus, OH, USA
- 88 Physics department, Faculty of science, University of Zagreb, Zagreb, Croatia
- 89 Physics Department, Panjab University, Chandigarh, India
- 90 Physics Department, University of Jammu, Jammu, India
- 91 Hiroshima University, Hiroshima, Japan
- 92 Physikalisches Institut, Eberhard-Karls-Universität Tübingen, Tübingen, Germany
- 93 Physikalisches Institut, Ruprecht-Karls-Universität Heidelberg, Heidelberg, Germany
- 94 Physik Department, Technische Universität München, Munich, Germany
- 95 Politecnico di Bari and Sezione INFN, Bari, Italy
- 96 Research Division and ExtreMe Matter Institute EMMI, GSI Helmholtzzentrum für Schwerionenforschung GmbH, Darmstadt, Germany

- 97 Saga University, Saga, Japan
- 98 Saha Institute of Nuclear Physics, Homi Bhabha National Institute, Kolkata, India
- 99 School of Physics and Astronomy, University of Birmingham, Birmingham, UK
- 100 Sección Física, Departamento de Ciencias, Pontificia Universidad Católica del Perú, Lima, Peru
- 101 Stefan Meyer Institut für Subatomare Physik (SMI), Vienna, Austria
- 102 SUBATECH, IMT Atlantique, CNRS-IN2P3, Nantes Université, Nantes, France
- 103 Sungkyunkwan University, Suwon City, Republic of Korea
- 104 Suranaree University of Technology, Nakhon Ratchasima, Thailand
- 105 Technical University of Košice, Košice, Slovak Republic
- 106 The Henryk Niewodniczanski Institute of Nuclear Physics, Polish Academy of Sciences, Cracow, Poland
- 107 The University of Texas at Austin, Austin, TX, USA
- 108 Universidad Autónoma de Sinaloa, Culiacán, Mexico
- 109 Universidade de São Paulo (USP), São Paulo, Brazil
- 110 Universidade Estadual de Campinas (UNICAMP), Campinas, Brazil
- 111 Universidade Federal do ABC, Santo Andre, Brazil
- 112 Universitatea Nationala de Stiinta si Tehnologie Politehnica Bucuresti, Bucharest, Romania
- 113 University of Derby, Derby, UK
- 114 University of Houston, Houston, TX, USA
- 115 University of Jyväskylä, Jyväskylä, Finland
- 116 University of Kansas, Lawrence, KS, USA
- 117 University of Liverpool, Liverpool, UK
- 118 University of Science and Technology of China, Hefei, China
- 119 University of South-Eastern Norway, Kongsberg, Norway
- 120 University of Tennessee, Knoxville, TNN, USA
- 121 University of the Witwatersrand, Johannesburg, South Africa
- 122 University of Tokyo, Tokyo, Japan
- 123 University of Tsukuba, Tsukuba, Japan
- 124 Universität Münster, Institut für Kernphysik, Münster, Germany
- 125 CNRS/IN2P3, LPC, Université Clermont Auvergne, Clermont-Ferrand, France
- 126 Institut de Physique des 2 Infinis de Lyon, CNRS/IN2P3, Université de Lyon, Lyon, France
- 127 CNRS, IPHC UMR 7178, Université de Strasbourg, 67000 Strasbourg, France
- 128 Département de Physique Nucléaire (DPhN), Centre d'Etudes de Saclay (CEA), IRFU, Université Paris-Saclay, Saclay, France
- 129 CNRS/IN2P3, IJCLab, Université Paris-Saclay, Orsay, France
- 130 Università degli Studi di Foggia, Foggia, Italy
- 131 Università del Piemonte Orientale, Vercelli, Italy
- 132 Università di Brescia, Brescia, Italy
- 133 Variable Energy Cyclotron Centre, Homi Bhabha National Institute, Kolkata, India
- 134 Warsaw University of Technology, Warsaw, Poland
- 135 Wayne State University, Detroit, MI, USA
- 136 Yale University, New Haven, CT, USA
- 137 Yildiz Technical University, Istanbul, Turkey
- 138 Yonsei University, Seoul, Republic of Korea
- 139 Affiliated with an Institute Formerly Covered by a Cooperation Agreement with CERN, Geneva, Switzerland
- 140 Affiliated with an International Laboratory Covered by a Cooperation Agreement with CERN, Geneva, Switzerland
- ^a Also at: Max-Planck-Institut für Physik, Munich, Germany
- ^b Also at: Italian National Agency for New Technologies, Energy and Sustainable Economic Development (ENEA), Bologna, Italy
- ^c Also at: Dipartimento DET del Politecnico di Torino, Turin, Italy

^d Also at: Department of Applied Physics, Aligarh Muslim University, Aligarh, India

^e Also at: Institute of Theoretical Physics, University of Wrocław, Wrocław, Poland

^f Also at: Facultad de Ciencias, Universidad Nacional Autónoma de México, Mexico City, Mexico

* Deceased